Cretaceous Research 39 (2013) 149–169

Contents lists available at SciVerse ScienceDirect

Cretaceous Research

journal homepage: www.elsevier.com/locate/CretRes

Stratigraphic framework and calcareous nannofossil productivity of the Essaouira-Agadir Basin (Morocco) during the Aptian–Early Albian: Comparison with the north-Tethyan margin

C. Peybernes [a,b], F. Giraud [b,*], E. Jaillard [b], E. Robert [b], M. Masrour [c], M. Aoutem [c], N. Içame [c]

[a] UMR 5276 CNRS Laboratoire de Géologie de Lyon Terre Planètes Environnement, Université Lyon 1-ENS Lyon, Bâtiment Géode, 2 rue Raphaël Dubois, 69622 Villeurbanne cedex, France
[b] ISTerre, Université de Grenoble 1, UMR 5275 CNRS and IRD, F-38041 Grenoble, France
[c] Université Ibn Zohr, Faculté des Sciences, Département de Géologie, B.P. 8106, Cité Dakhla, Agadir, Morocco

ARTICLE INFO

Article history:
Received 26 April 2011
Accepted in revised form 28 February 2012
Available online 26 April 2012

Keywords:
Southern Tethyan margin
Ammonite biostratigraphy
Sedimentary correlations
Carbonate production
Calcareous nannofossil fluxes
Trophic conditions

ABSTRACT

In the southern Tethyan margin, the Essaouira-Agadir Basin (EAB), south of Morocco, exhibits well-exposed and fossiliferous sections of Aptian–Albian age. Biostratigraphy by ammonoids and sedimentological analysis have been realized for five sections located along an E-W transect in the EAB. The studied successions were dated from the latest Early Aptian to the Early Albian and are characterized by five major sedimentary discontinuities defining at least four main sedimentary sequences. The Late Aptian–Early Albian succession can be considered a gently westward-dipping ramp, marked by a deepening upward evolution. A quantitative study of calcareous nannofossils and calcium carbonate content has been performed on three of these sections. At this time, the EAB was located in the tropical-equatorial hot arid belt. The decrease in both calcium carbonate content and *Nannoconus* abundances at the Aptian–Albian transition could be the result of cooler climatic conditions recognized in the EAB, and/or of the associated increasing terrigenous input and nutrients, which hindered carbonate production. In the EAB, the nannofossil productivity is higher below the deposition of dark levels, which are coeval with the Niveau Paquier, recognized as the expression in southern France of the OAE 1b (Early Albian). During the Early Albian, the EAB was characterized by nannofossil fluxes two times lower than the upwelling-influenced Mazagan Plateau (southern Tethyan margin) and eight times lower than the Vocontian Basin (northern Tethyan margin). These results show that, with respect to the northern Tethyan margin, trophic conditions in sea surface waters of the pelagic realm of the southern Tethyan margin were lower. Comparable results obtained by Heldt et al. in the neritic realm of the southern Tethyan margin have been ascribed to more arid climatic conditions.

1. Introduction

In terms of global changes, the Aptian–Early Albian time interval was a period of (1) increasing oceanic accretion with the opening of the Western Mediterranean sea and the rifting of the Central Atlantic Ocean, (2) eustatic sea-level rise, (3) deposition of black shales in oceanic settings, expression of two "Oceanic Anoxic Events" (OAEs, Schlanger and Jenkyns, 1976; Arthur et al., 1990; Bralower et al., 1994) and (4) climatic changes characterized by successive brief episodes (<1 my–5 my) of warming and cooling (Frakes and Francis, 1988; Weissert and Lini, 1991; Price, 2003; Pucéat et al., 2003; Weissert and Erba, 2004; Takashima et al., 2007; Wagner et al., 2008; Ando et al., 2008; Kuhnt et al., 2011). These OAEs are associated with major excursions of $\delta^{13}C$. The Early Aptian OAE 1a is marked by a major negative excursion, preceding the deposition of black shale, followed by a long-term $\delta^{13}C$ positive shift (Menegatti et al., 1998). The OAE 1b is characterized by a distinct negative shift in various carbon reservoirs coincident with the black shale (Herrle et al., 2004; Wagner et al., 2007).

During this time interval, major changes in the carbonate production affected especially the (sub)tropical platforms located on the northern Tethyan passive margin both during climatic warmings, as the Early Aptian with the OAE 1a, and during climatic coolings as those recorded at the Late Aptian–Early Albian

* Corresponding author. ISTerre, Université de Grenoble 1, Maison des Géosciences, 1381 rue de la Piscine, BP 53, 38041 Grenoble cedex 9, France. Tel.: +33 (0) 4 76 51 40 73; fax: +33 (0) 4 76 63 52 01.
E-mail address: Fabienne.Giraud-Guillot@ujf-grenoble.fr (F. Giraud).

0195-6671/$ – see front matter © 2012 Elsevier Ltd. All rights reserved.
doi:10.1016/j.cretres.2012.02.017

transition (Weissert and Lini, 1991; Herrle and Mutterlose, 2003; Heimhofer et al., 2008; Mutterlose et al., 2009). Among different hypotheses, some authors proposed that enhanced terrigenous influx combined with sea-level rise would have brought more nutrients in the sea surface waters of the oceanic realm. The effects of eutrophication on the carbonate platforms are drastic changes in biological communities and a reduction of the carbonate productivity (Hallock and Schlager, 1986; Wood, 1993; Mutti and Hallock, 2003; Pittet et al., 2002). These biotic changes usually precede the drowning of carbonate platforms on the northern Tethyan margins.

Various studies show that the major carbonate crisis recorded on the carbonate platforms of the northern Tethyan margin during the Early Aptian (OAE 1a, Weissert et al., 1998; Wissler et al., 2003; Föllmi et al., 2006) is not recorded in the shallow paleoenvironments of the southern Tethyan margin (Oman, Immenhauser et al., 2005; Egypt, Thielemann, 2006; Tunisia, Heldt et al., 2008). The calcium carbonate content measured in the sediments of these platforms remains high even during intervals of major perturbations as the OAE 1a. Focusing on the Tunisian carbonate platform, Heldt et al. (2010) show that no widespread platform drowning is recorded at this time, possibly due to non-eutrophication of this platform located within the broad arid climate belt of Chumakov et al. (1995).

In the oceanic realm, trophic conditions prevailing in sea surface can be depicted by quantifying calcareous nannofossil fluxes and assemblages.

The Aptian–Albian time interval is a key period in the evolution of calcareous planktonic organisms, generally linked with major Oceanic Anoxic Events recognized in oceanic settings (OAE 1a: Early Aptian; OAE 1b: Early Albian). Changes in nannofossil assemblages precede or follow the OAE. The planktonic foraminifera display an important radiation after the OAE 1a, characterized by a large variability of both size and morphology of the tests, leading to a significant increase of the species diversity (*e.g.* Leckie et al., 2002; Huber and Leckie, 2011). Significant decrease in the nannofossil species richness and important rates of turnover and diversification are recorded, coincident with the Early Albian OAE 1b (Bralower et al., 1993).

So far, nannofossil quantitative studies including absolute abundance and assemblages have been performed in the northern Tethyan margin (Vocontian Basin sections) on the Kilian (Late Aptian) and the Paquier (OAE 1b, Early Albian) levels, respectively, and in the southern Tethyan margin (DSDP site 545, Mazagan Plateau) on the OAE 1b (Herrle, 2002). Herrle (2002) showed that the fertility of sea surface waters was higher in the Vocontian Basin than in the Mazagan Plateau, possibly due to a more humid climate.

In the southern Tethyan margin, the Essaouira-Agadir Basin (EAB), south of Morocco, is characterized by fossiliferous stratigraphic sections of Aptian–Early Albian age. Among several studied sections correlated thanks to ammonite biostratigraphy and recognition of major sedimentary unconformities, we performed quantitative study of calcareous nannofossil assemblages and calcium carbonate content on three sections of this basin. The nannofossil productivity results are compared with those obtained by Herrle (2002) for the Mazagan Plateau and the Vocontian Basin.

2. Geological setting

The Essaouira-Agadir Basin (EAB) is part of the African passive margin of the Central Atlantic Ocean (Coward and Ries, 2003; Zühlke et al., 2004; Hafid et al., 2008). Atlantic rifting started in the Late Permian–Triassic, and culminated with the initiation of oceanic accretion in the Middle Jurassic (Hafid, 2000; Le Roy and Piqué, 2001). This was followed by a phase of thermal subsidence, combined with well-recorded eustatic transgressions (LeRoy et al., 1998). Passive margin evolution ended in the Late Cretaceous with the onset of compressional deformations, which culminated in the Late Eocene–Oligocene and in the Pliocene, with the Atlasic orogeny (Frizon de la Motte et al., 2000, 2008). The folded sedimentary pile of the EAB is presently included in the Western High Atlas Chain (Fig. 1A).

Pioneer works on the Cretaceous stratigraphy of the EAB are due to Roch (1930), Ambroggi (1963) and Duffaud et al. (1966). These workers described the macro- and micro-fauna, and established the stratigraphy of the Cretaceous succession of the EAB; their nomenclature and age assignments are still in use. Later on, numerous local biostratigraphic and sedimentologic works led to the publication of refined stratigraphic data (Wiedmann et al., 1978; Canérot et al., 1986; Rey et al., 1988; Andreu, 1989, 1992; Bourgeoini, 1994; Witam, 1998; Bourgeoini et al., 2002), sedimentary sequence successions (Canérot et al., 1986; Rey et al., 1988; Andreu, 1989; Algouti et al., 1999), detailed sedimentologic studies on the Barremian (Nouidar and Chellaï, 2001, 2002) or the Cenomanian–Turonian interval (Ettachfini and Andreu, 2004; Ettachfini et al., 2005; Jati et al., 2010), and paleontological or paleobiogeographic synthesis (Middlemiss, 1980; Andreu, 1992; Wippich, 2003; Masrour et al., 2004; Company et al., 2008). Meanwhile, thanks to petroleum and oceanographic explorations, the offshore part of the EAB has been explored, leading to a comprehensive understanding of this basin (Leckie, 1984; Broughton and Trepanier, 1993; Hafid et al., 2000; Herrle, 2002; Mehdi et al., 2004; Zühlke et al., 2004; Davison, 2005; Hofmann et al., 2008; Davison and Davy, 2010).

The rifting phase gave way to the deposition of thick red bed deposits of Late Permian–Triassic age, overlain by a thick series of shales and evaporites intercalated with basaltic flows dated as early Liassic (Hafid et al., 2000). The drifting period (from late Liassic onwards) coincides with the onset of low thermal subsidence of the margin (Bouatmani et al., 2007) and with the development of a widespread, shallow marine carbonate platform, and deeper marine carbonates to the West (Zühlke et al., 2004; Hafid et al., 2008).

The Cretaceous transgression followed a sharp regression of latest Jurassic age (Zühlke et al., 2004). A first cycle began with Berriasian shelf limestones and reached a maximum within Valanginian, open marine marls (Rey et al., 1988; Masrour et al., 2004). Hauterivian sediments are marked by shallowing upward deposits, which are overlain by inner shelf limestones or fluvial sandstones of Late Hauterivian–Barremian age (Canérot et al., 1986; Witam, 1998). A second cycle is represented at the base by Aptian shelf limestones that grade upwards into open marine shales of Albian age, which are in turn overlain by shallow marine marls and limestones, or even sandstones, of latest Albian age (Butt, 1982; Essafraoui et al., 2010). Upper Cretaceous times are then marked by two more transgressive–regressive cyles, one of Cenomanian–Turonian age, marked by a regional discontinuity at the Cenomanian/Turonian boundary (Ettachfini et al., 2005; Jati et al., 2010), and the other one of Senonian age, which is marked by a compressional teconic event of Campanian age (Algouti et al., 1999).

Salt tectonic and diapir activity began in the Jurassic and occurred repeatedly during the Cretaceous, controlling largely facies distribution in the distal, offshore part of the Basin (Tari et al., 2000; Mehdi et al., 2004; Zühlke et al., 2004).

Although parts of the Cretaceous succession have been studied in detail (e.g. Nouidar and Chellaï, 2001, 2002; Jati et al., 2010), the Late Aptian–Albian transgression is still poorly understood, because of the thick, monotonous and poorly fossiliferous shaly succession that represent most of the Albian stage. We studied five sections located along a roughly East-West transect of the margin, little North of the Agadir city. From East to West, these sections are: Tinfoul, Tamzergout, Alma, Addar and Tamri (Fig. 1B).

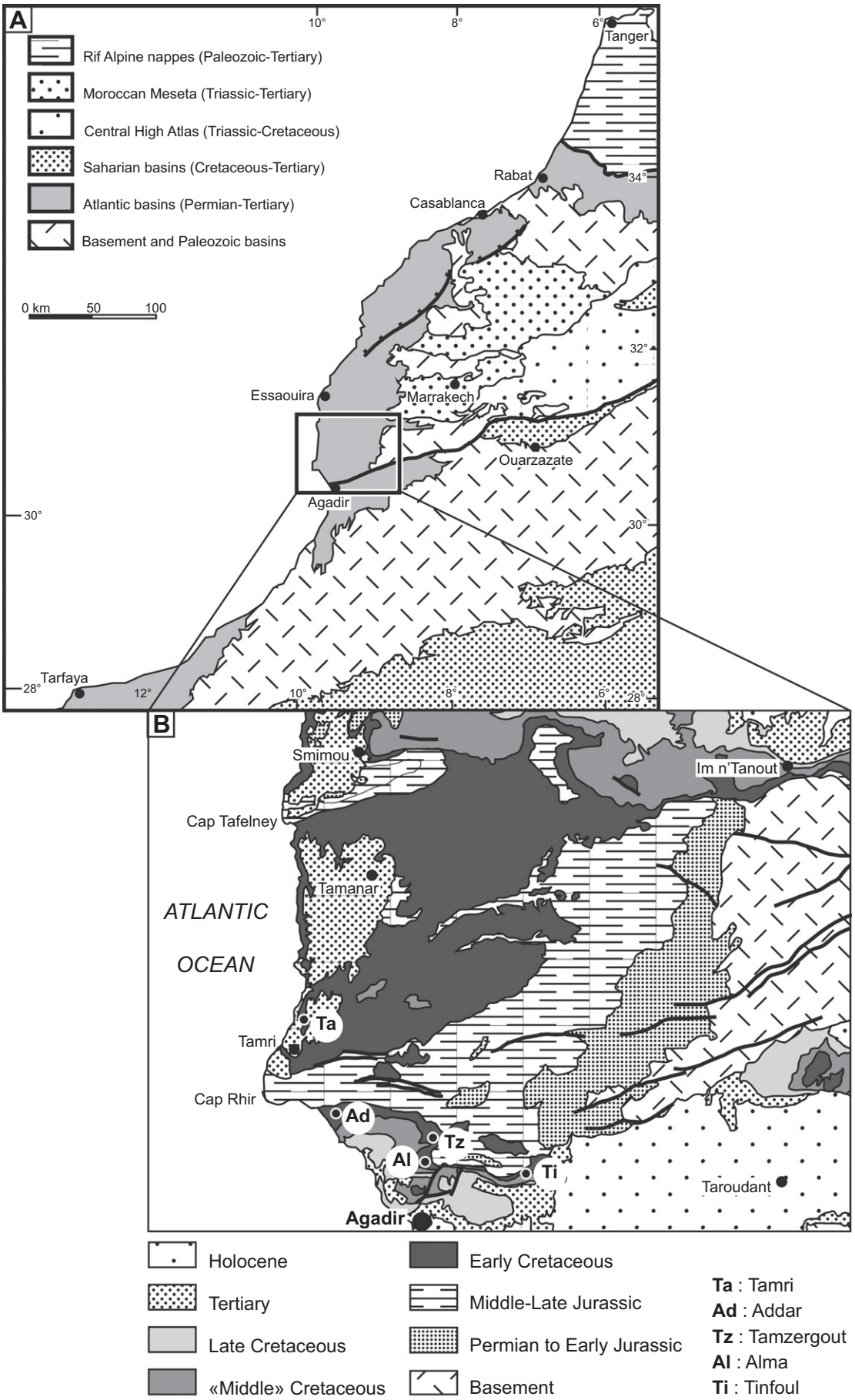

Fig. 1. Location maps (simplified from Zühlke et al., 2004). A: structural sketch of Western Morocco. B: Geological map of the Essaouira-Agadir Basin, and location of the sections discussed in the text.

3. Methods

3.1. Ammonites

In its present stage, our study includes about 1500 specimens of ammonites collected during the years 2008 and 2009 from eight Aptian–Early Albian stratigraphic sections in the EAB. Ammonites are unequally distributed throughout the studied interval; lowermost Early Aptian beds and upper Lower Albian marls yielded scarce material whereas the median part (uppermost Aptian to basal Albian) contains abundant material. The ammonite distribution has been studied through bed by bed sampling.

Collected material has been compared with specimens of the South Moroccan collections (Gentil, Kilian, Roch, Breistroffer), and other historical private Aptian–Albian specimens of the Mediterranean provinces, deposited in the "Institut Dolomieu collection" (Observatoire des Sciences de l'Univers, Grenoble University). Ammonite specimens collected during the present study have been deposited and referenced in the same collection.

Ammonites are preserved either as small pyritized molds, very abundant in the calcareous and argillaceous marls, or as internal calcareous molds in the more massive and calcareous beds. Comparison of the ontogeny of both kinds of material is sometimes difficult, especially for the adult stages.

3.2. Calcimetry and calcareous nannofossils

Fifty-seven samples collected from the three sections of Alma, Addar and Tamzergout were analyzed for calcium carbonate content and for calcareous nannofossils. Samples are usually selected from more favorable lithologies (argillaceous marls, marls, calcareous marls) for nannofossil studies, with a few number collected from limestones, in order to have a sampling representative of the various lithologies. Calcium carbonate content was determined using the carbonate bomb technique, which measures CO_2 emission during a hydrochloric acid attack. The calculation of the calcium carbonate percent is given in Appendix A.

Samples for nannofossil studies were prepared using the random settling technique of Geisen et al. (1999), a method adapted from Beaufort (1991) that allows calculate absolute abundances. This method is now applied in different studies focused on Cretaceous nannofossil assemblages allowing comparison of these assemblages between different settings (Herrle, 2002; Bornemann et al., 2003, 2005; Herrle et al., 2003; Reboulet et al., 2003; Hardas and Mutterlose, 2007; Linnert et al., 2010). Nannofossils were observed under a light polarizing microscope, at 1560× magnification. 300 specimens were generally counted in a variable number of fields of view on the smear slide. In the poorest nannofossil samples, 150 specimens were counted following one longitudinal transverse. The taxonomic framework of Burnett et al. (*in* Bown, 1998) is followed. The nannofossil preservation was evaluated following the classes defined by Roth (1983). Relative abundances of each species were also calculated for each sample. In the calculation of the relative abundance, *Nannoconus* are excluded from the total sum of nannofossils because of their uncertain biological affinity. Busson and Noël (1991) have compared the episodic proliferation of *Nannoconus* to those of extant dinoflagellates and proposed that they could be closely related groups. Aubry et al. (2005) in a reference work on the Mesozoic nannofossil size evolution did not take into account these nannoliths because of their uncertain biological and ecological affinities. The nannofossil assemblage composition can also be described by means of the species richness, the Shannon Diversity Index and evenness defined by Shannon and Weaver (1949). *Nannoconus* are excluded from these calculations as explained before. The relationships between the different paleoenvironmental proxies ($CaCO_3$ %, nannofossil absolute abundance, species richness, diversity and evenness, percentage of *Nannoconus*) were investigated by linear correlation (Correlation coefficient of Pearson). This correlation coefficient can be used only with variables showing a gaussian distribution. To respect this criterion, the nannofossil absolute abundance is normalized, in calculating the $\log arithm_{10}$ of each absolute abundance value. For each correlation coefficient, r, a statistical test for significance is computed ("Fisher's Z-transformation", Fisher, 1921).

Nannofossil absolute abundances are usually biased by dilution. Therefore, we calculated nannofossil fluxes. In addition, sedimentation rates were estimated by using time duration proposed by Herrle (2002). The nannofossil fluxes are expressed as:

$$F\,(\text{number of nannofossils per meter square and per year}) = AA^{*}\rho^{*}\text{sed. Rate}$$

with AA: nannofossil absolute abundance; ρ: volume mass of calcite (2.7 g cm^{-3}) and sed. Rate: sedimentation rate.

4. Results

4.1. Ammonite biostratigraphy

The Aptian and Albian ammonites of the EAB have been first reported respectively by Lemoine (1905) and Brives (1905). Gentil (1905), Kilian and Gentil (1906, 1907), and later Roch (1930), listed some faunas and proposed stratigraphic interpretations. Ambroggi (1963) published the first regional synthesis, which remains until today the reference for the understanding of biological and sedimentological chronologies of the basin.

Our analysis of the distribution of the ammonite species identified in the Aptian–Albian of the EAB allowed us to establish a detailed faunal succession. The preliminary state of our study does not allow us to propose a local zonation; we will develop it in a forthcoming publication. However, thanks to the presence of numerous Tethyan species, our succession can be easily correlated with the Standard Mediterranean Zonation proposed by IUGS Lower Cretaceous Ammonite Working Group ("Kilian Group"; Reboulet et al., 2011).

We were able to correlate the ammonite succession with the four Late Aptian standard zones and with the first two zones of the Lower Albian. The Early Aptian and basal Late Aptian zones have also been identified but with much less accuracy because of condensed sedimentation and temporal hiatuses. The zones are assemblage or interval zones, the bases of which are defined either by the first appearance of the index species, or by a diagnostic ammonite association that allows its identification even though the index species is lacking. Note that, since some assemblages occur in condensed beds and show mixed taxa, the interpretation of the biozones must be taken with caution.

Various new species and/or genus have been recognized in the ammonite faunas of the EAB. However, because the purpose of this section is to present our stratigraphic framework, these endemic species are not mentioned in the text and the table; they are only listed in Fig. 2.

Early Aptian

Resting on the Barremian massive sandy limestones, the Early Aptian to basal Late Aptian succession is marked by various sedimentary discontinuities and condensation levels. Ammonite specimens of Early Aptian age are scarce and poorly preserved, and ammonite zones are difficult to identify in this interval. They are not represented in the Tinfoul Section (Fig. 3).

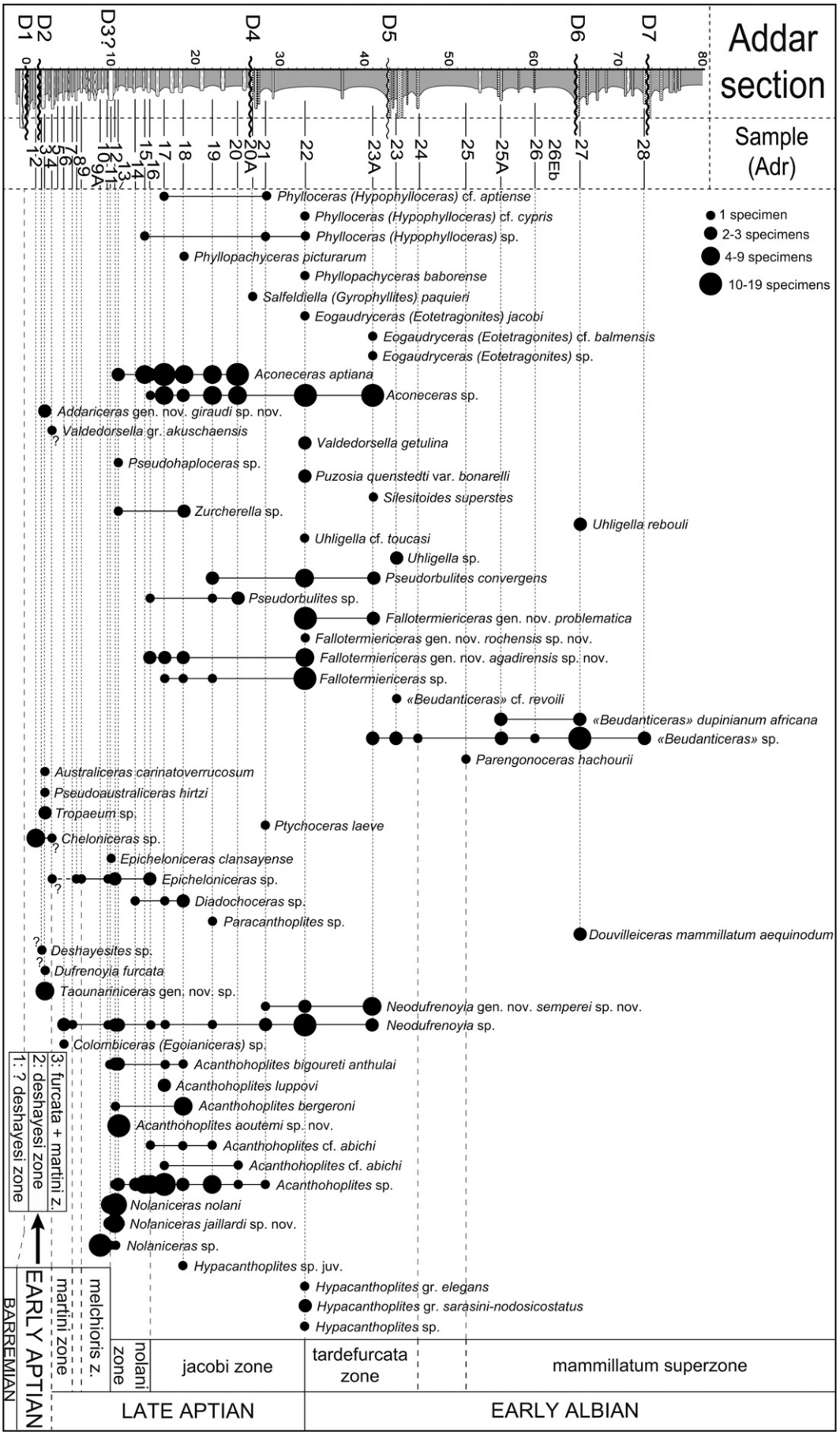

Fig. 2. Ammonite occurrences and standard biostratigraphic interpretation of the reference regional Addar section (for lithology, see caption of Fig. 4).

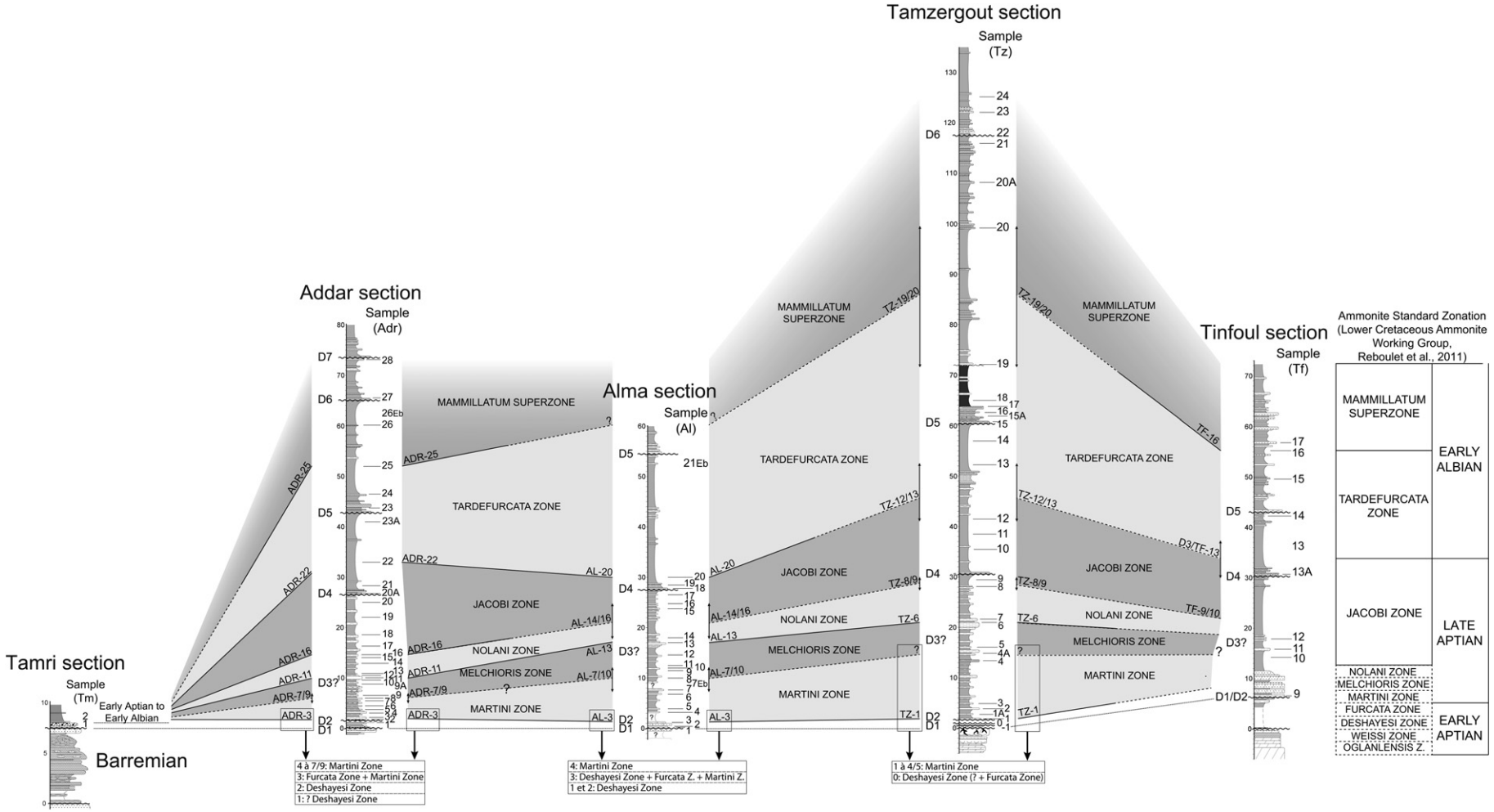

Fig. 3. Regional biostratigraphic correlations with standard zonation nomenclature across the studied sections of the EAB (for lithology, see caption of Fig. 4).

However, in Addar (Fig. 2), the occurrence of *Cheloniceras* sp. (bed 1) and *Deshayesites* sp. indicates an uppermost Early Aptian age. These genera are possible markers of the *Deshayesites deshayesi* Zone. This assignment is supported by the occurrence of other representatives of the genus *Deshayesites* (Table 1).

The *Dufrenoyia furcata* Zone has been recognized in various sections. However, these species co-occur in the same beds with taxa indicative of the overlying *Epicheloniceras martini* Zone of basal Late Aptian age. This mixing of taxa corroborates the condensation of the succession and the amalgamation of discontinuities.

Late Aptian

The Late Aptian zones are better identified than the Early Aptian ones, except in the Tinfoul section, where only the *Hypacanthoplites jacobi* Zone is recognized.

Various ammonite species characteristic of the *Epicheloniceras martini* Zone are recognized (Table 1).

The identification of the *Parahoplites melchioris* Zone is more problematic; the index species is absent and other ammonites attributable to this zone are very scarce. As a consequence, the exact position of the lower boundary is uncertain (Fig. 3). We placed it at the first appearance of *Acanthohoplites* sp. (beds 9 in Addar and 10 in Alma), where it is associated with *Colombiceras discoidale* Sinzow.

The overlying *Acanthohoplites nolani* Zone is well recognized in all the studied sections; the "*nolani* beds" define a very characteristic horizon, known since early publications. Its lower boundary is placed at the first appearance of the index species, associated with other *Acanthohoplites* species (Table 1).

The *Hypacanthoplites jacobi* Zone has also been recognized in all sections, even though the index species is absent in our material; the genus *Hypacanthoplites* is moreover little represented in the ammonite assemblages of the zone, although Acanthohoplitinae dominate. The lower boundary is also not well defined in the Alma and Tamzergout sections, and we conventionally placed it at the first appearance of *Pseudorbulites* sp. (bed 16 in Addar).

Earliest Albian

The Aptian/Albian boundary is still in debate (e.g. Owen, 1984; Huber and Leckie, 2011). Partly due to the high provincialism, which prevents interregional correlations (Huber and Leckie, 2011), the ammonite fauna is of little help, so far, to define the base of the Albian stage, especially on the southern margin of the Tethys (Latil *in* Chihaoui et al., 2010; Latil, 2011). Nevertheless, the presence of cosmopolitan taxa in the Moroccan faunas can greatly improve correlations with the standard Western Europe ammonite biozonation and may provide new insights on the definition of the base of the Albian stage.

The *Leymeriella tardefurcata* Zone is identified in all the studied sections, even though the index species is absent as in the entire Mediterranean region. Characteristic species have been recorded for the zone (Table 1). Until now, the Aptian/Albian boundary cannot be determined accurately in the Tamzergout and Tinfoul sections (Fig. 3).

The *Douvilleiceras mammillatum* Superzone has been identified in the uppermost part of the studied successions, with the exception of the Alma Section where it has not been recognized (Fig. 3). Its lower boundary is difficult to determine in various sections, except in the Addar and Tinfoul sections, which record the respective occurrences of *Parengonoceras hachourii* (Dubourdieu, 1953) and *Douvilleiceras mammillatum aequinodum* (Quenstedt). Ammonite assemblages comprising numerous specimens of the genus "*Beudanticeras*" (Table 1), define the very characteristic "*Beudanticeras* beds" horizon of the historical literature (Roch, 1930; Ambroggi, 1963).

The Aptian and Early Albian are reduced to a phosphatic crust in the Tamri area (Fig. 1B). This hardground yielded an ammonite assemblage comprising species characteristic of the Early Aptian (e.g. *Cheloniceras* gr. *cornuelianum* (d'Orbigny), *C.* gr. *meyendorfi-seminodosum*, *Toxoceratoides* sp.), the Late Aptian (*Deshayesites* sp., *Dufrenoyia dufrenoyi* (d'Orbigny), *Colombiceras* sp., *Vectisites caprotinus* Casey), the Late Aptian–Early Albian interval (*Pseudorbulites* sp., *Puzosia* sp.) and the Albian (*Uhligella* cf. *rebouli* (Jacob) and *Engonoceras* sp.) (Fig. 3).

4.2. Sedimentary correlations

As a whole, the Late Aptian–Early Albian succession does not present any high energy and barrier facies and can be considered a westward, gently dipping ramp, marked by a deepening upward evolution that documents the Late Aptian–Early Albian eustatic transgression. Since detailed sedimentological analysis is not yet achieved, we will only describe the identified unconformities, which allow us to specify the biostratigraphic correlations.

Five main discontinuities have been recognized, which are correlatable in all the studied sections, thus defining at least four main sedimentary sequences (Fig. 4). Note, that in the westernmost Tamri section, these five discontinuities are contained within a single, 50 cm-thick, conglomeratic phosphatic hardground.

Table 1
Ammonite associations identified in the studied sections (Essaouira-Agadir Basin), and correlations with the Early Aptian to Early Albian Standard Ammonite Zones.

Substages	Ammonite standard zones	Ammonite associations
Early Albian	*Douvilleiceras mammillatum*	*Beudanticeras dupinianum africana* Pervinquière, *Beudanticeras revoili* Pervinquière, *Uhligella rebouli* Jacob, *Parengonoceras hachourii* Dubourdieu, *Douvilleiceras mammillatum aequinodum* Quenstedt
	Leymeriella tardefurcata	*Phylloceras (Hypophylloceras)* cf. *cypris* Fallot & Termier, *Phyllopachyceras baborense* (Coquand), *Eogaudryceras (Eotetragonites)* cf. *balmensis* Breistroffer, *Valdedorsella getulina* (Coquand), *Puzosia (Puzosia) quenstedti* (Parona & Bonarelli), *Puzosia (Puzosia) quenstedti bonarelli* Breistroffer *in* Besairie, *"Uhligella"* cf. *toucasi* (Jacob), *"Beudanticeras"* cf. *revoili* (Pervinquière), *Oxytropidoceras (Oxytropidoceras)* sp., *Silesitoides superstes* (Jacob), *Neosilesites palmensis* (Fallot & Termier), *"Hypacanthoplites" numidiscus* (Sornay), *Hypacanthoplites elegans* (Fritel), *Hypacanthoplites* gr. *sarasini-nodosicostatus*
Late Aptian	*Hypacanthoplites jacobi*	*Phylloceras (Phylloceras) aptiense* Sayn, *Phyllopachyceras picturarum* (d'Orbigny), *Aconeceras aptiana* (Sarasin), *Pseudorbulites convergens* (Jacob), *Diadochoceras migneni* (Seunes), numerous *Acanthohoplites*, *Hypacanthoplites nolaniformis* (Glazunova), *Epicheloniceras clansayense* (Jacob)
	Acanthohoplites nolani	*Aconeceras aptiana* (Sarasin), *Pseudohaploceras* sp., *Zuercherella* sp., *Acanthohoplites nolani* (Seunes), *Acanthohoplites bigoureti anthulai* Breistroffer, *Acanthohoplites bergeroni* (Seunes), *Epicheloniceras clansayense* (Jacob), *Diadochoceras* sp.
	Parahoplites melchioris	*Acanthohoplites* sp., *Colombiceras discoidale* (Sinzow)
	Epicheloniceras martini	*Epicheloniceras martini* (d'Orbigny), *Colombiceras (Egoianiceras)* sp., *Colombiceras* sp., *Pseudoaustraliceras hirtzi* Collignon, *Australiceras* sp. (= *Tropaeum* in regional literature)
Early Aptian	*Dufrenoyia furcata*	*Dufrenoyia furcata* (Sowerby), *Tropaeum* sp., *Toxoceratoides emericianum* (d'Orbigny)
	Deshayesites deshayesi	*Cheloniceras* sp., *Deshayesites deshayesi* (d'Orbigny *in* Leymerie), *Deshayesites consobrinoides* (Sinzow)

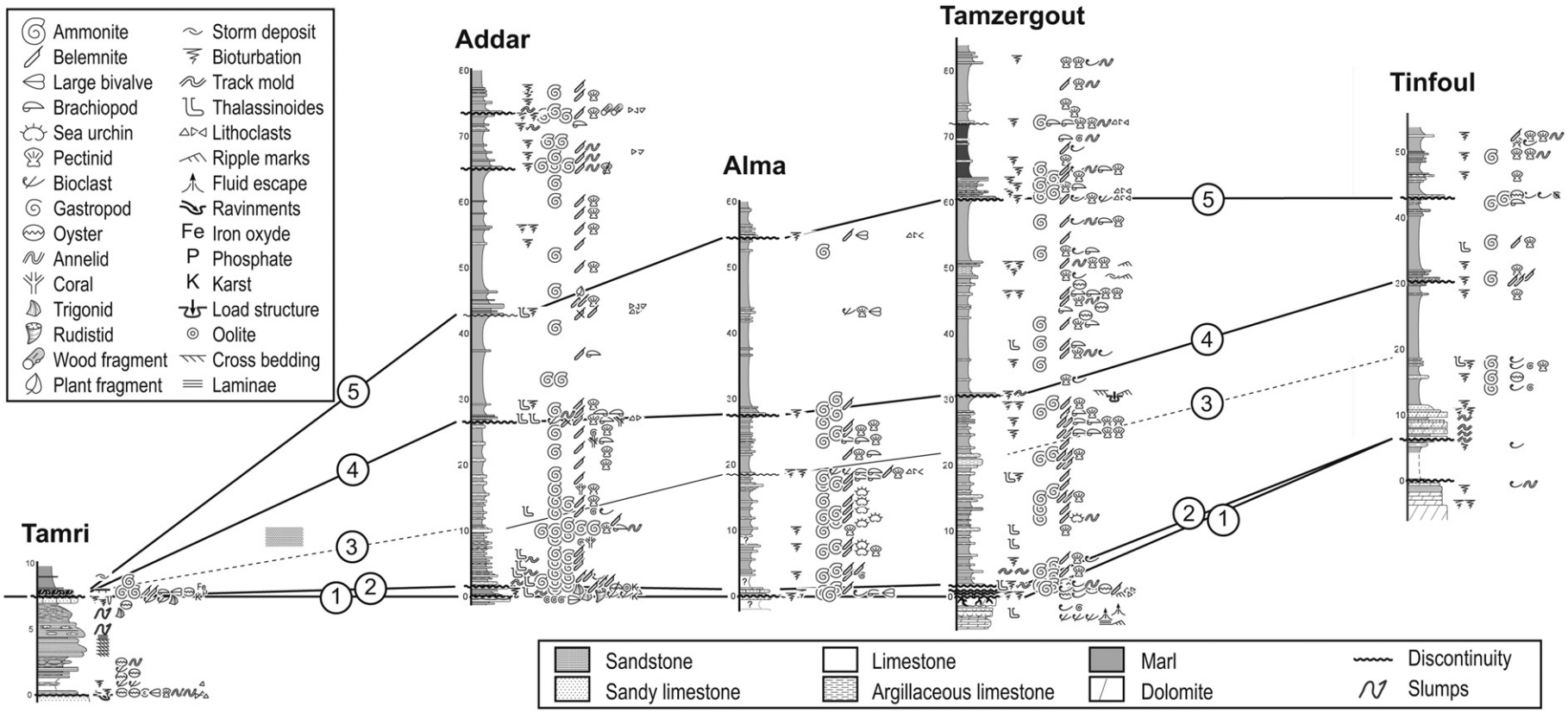

Fig. 4. Main discontinuities identified in the Late Aptian–Early Albian interval of the southern part of the Essaouira-Agadir Basin. Sections are located on Fig. 1B.

The first discontinuity is located at the top of the Barremian massive limestones or sandstones. It is marked, according to the sites, by a karstified surface (Tamzergout, Addar, Tinfoul), by an erosional surface (Alma), or by a simple, abrupt, lithological change (Tinfoul).

The second discontinuity is either amalgamated with the first one (Tamri, Alma, Tinfoul), or located 1 m, or less, above the first one. It consists of either an erosional surface (Tamzergout), or a karstified surface (Addar). The second unconformity overlies scarce ammonites that indicate a late Early Aptian age (*Deshayesites deshayesi* Zone (and *Dufrenoyia furcata* Zone)). Although observations are scarce and difficult (strong diagenesis), the associated fauna indicates a shallow marine depositional environment.

A third discontinuity seems to be located within the "Nolani Beds". It is marked by an erosional surface overlain by reworked clasts (Alma) or by a condensed, bioturbated surface marked by ammonite accumulations (Addar). It has not been clearly observed as yet in the Tamri, Tamzergout and Tinfoul sections. Since it lies within the "Nolani Beds", it is of Late Aptian age.

The fourth discontinuity is marked by a very constant layer of reddish sandstone that contains commonly green phosphatic, and reworked clasts and fossil fragments (Addar, Alma, Tinfoul), and probably corresponds to a submarine hiatus. The underlying sequence is of latest Aptian age (*Hypacanthoplites jacobi* Zone), and was deposited in an open marine, deep outer shelf, as suggested by the scarce benthic fauna (brachiopods, pectinids and other bivalves).

The fifth discontinuity roughly coincides with the base of the "Beudanticeras Beds". It is marked by a constant bed of yellow sandstone that reworks white phosphatic clasts, ammonite fragments, and shaly flat pebbles, thus documenting a sedimentary hiatus and a period of submarine erosion. The underlying series is virtually devoid of benthic fauna in the western sections (Addar, Alma), and contains abundant brachiopods, pectinids and annelids in the eastern sections, thus documenting a basin to outer shelf environment. Overlying ammonite assemblages indicate an earliest Albian age (*Leymeriella tardefurcata* Zone).

The overlying marly series contains several beds of sandstones with erosional base, which probably represent additional discontinuities. Available biostratigraphic data indicate an Early to Late Albian age (Ambroggi, 1963; Duffaud et al., 1966; Rey et al., 1988).

4.3. Calcium carbonate content and calcareous nannofossils

All nannofossil taxa observed in the studied sections are reported in Appendix B. The nannofossil total assemblage is composed of 78 species. Some taxa that exhibit similar morphology have been grouped. *Biscutum* spp. includes *B. constans* and *B. ellipticum* (they belong to the same morphological continuum as demonstrated by Bornemann and Mutterlose, 2006). The *Cretarhabdus* group includes all species of the genera *Cretarhabdus* and *Retecapsa* (Roth and Krumbach, 1986). Nannoconids are grouped into *Nannoconus* spp. (Roth and Krumbach, 1986; Herrle et al., 2003). *Staurolithites* spp. include *S. mutterlosei*, *S. seisseri*, *S. imbricatus* and *S. mitcheneri*. All zeugrhabdotids (including *Z. erectus*) with major axis smaller than 5 μm are combined under small *Zeugrhabdotus* (Erba et al., 1992). *Watznaueria barnesiae* and *W. fossacincta* are lumped together because they are believed to represent end-members of a morphological continuum (Lees et al., 2004, 2006; Bornemann and Mutterlose, 2006).

4.3.1. The Alma section

The Alma section presents the oldest sediments among the three sections selected for calcium carbonate and nannofossil analysis (Fig. 5). The carbonate content varies from 24 to 79% except in the three first samples of the succession, which present values below 10%. Six samples are barren of nannofossils. Eight samples display moderately preserved nannofossils with moderate etching and overgrowth (categories E2 and O2) and three samples show poorly preserved specimens with strong etching and moderate overgrowth or moderate etching and strong overgrowth (categories E3/O2 or E2/O3).

The nannofossil absolute abundance ranges from 2.75×10^7 to 7.76×10^8 specimens per gram of sediment. The species richness varies from 11 to 31. The Shannon index and evenness range between 2.93–3.96, and 0.732–0.849, respectively. Lowest values are associated with poorly-preserved samples. Nine species or group of species are well represented in the assemblages and display important abundance fluctuations; they are in decreasing order of abundance: *Watznaueria barnesiae* (average value (av. v.) of 28.8%, maximum value (max. v.) of 43.2%), small *Zeugrhabdotus* (av. v. 10%, max. v. 13.4%) *Discorhabdus rotatorius* (av. v. of 9%, max. v. of 14.3%), *Biscutum* spp. (av. v. of 6.7%, max. v. of 15.7%), *Rhagodiscus asper* (av. v. of 5.9%, max. v. of 10.7%), *Watznaueria communis* (av. v. of 3.9%, max. v. of 6.9%), *Orastrum perspicuum* (av. v. of 3.9%, max. v. of 8%), *Nannoconus* spp. (av. v. of 3.4%, max. v. of 7.8%), *Lithraphidites carniolensis* (av. v. of 1.8%, max. v. of 4.6%). *W. barnesiae* and *D. rotatorius* generally do not present the same patterns for their absolute and relative abundances. Regarding the other taxa, their absolute and relative abundances follow the same trend. There is a decrease in both the absolute and relative abundances of *Nannoconus* spp. upward this short succession.

4.3.2. The Addar section

This section presents the most complete stratigraphic succession (Fig. 6). The calcium carbonate content varies between 30 and 56.5% at the base of the section, and progressively decreases upwards, to reach values around 10% (minimum of 7.6%).

Among the 27 selected samples, 6 samples are poorly preserved (categories E3/O2 or E2/O3), 13 samples are moderately preserved (categories E2 and O2) and 7 samples display well-preserved nannofossils with slight etching and overgrowth (categories E1 and O1). The nannofossil absolute abundance ranges from 3.81×10^7 to 2.44×10^9 specimens per gram of sediment. Highest abundances are recorded at the base of the section, and the absolute abundance decreases upward following the same trend as the carbonate content. Very low absolute abundances generally correspond to argillaceous sediments (carbonate content below 10%). The species richness varies from 15 to 35. The Shannon index and evenness fluctuate between 2.49–4.36, and 0.61–0.87, respectively. Variations of the nannofossil diversity are low except in the last 3 m of the succession. Ten species or group of species are well represented in the assemblages and display important abundance fluctuations; they are in decreasing order of abundance: *W. barnesiae* (av. v. of 26.2%, max. v. of 59%), small *Zeugrhabdotus* (av. v. of 10.7%, max. v. of 15.1%), *Biscutum* spp. (av. v. of 8.8%, max. v. of 16.8%), *D. rotatorius* (av. v. of 6.5%, max. v. of 12.3%), *R. asper* (av. v. of 4.7%, max. v. of 9.8%), *W. communis* (av. v. of 4.6%, max. v. of 13.8%), *Repagulum parvidentatum* (av. v. of 3.08%, max. v. of 15.7%), *L. carniolensis* (av. v. of 2.5%, max. v. of 5.8%), *O. perspicuum* (av. v. of 1.5%, max. v. of 9%), *Nannoconus* spp. (av. v. of 1.3%, max. v. of 5.5%). The relative abundances of *W. barnesiae* do not present the same pattern as their absolute abundances. For all other taxa, the absolute and relative abundances follow the same trend. The relative abundances of *Biscutum* spp. increase in the upper part of the section. *W. communis* is especially present at the base of the section. *R. parvidentatum*, which is not present in the Alma section, displays an increase in both absolute and relative abundances along the succession before to decrease gently at the top. The increase of

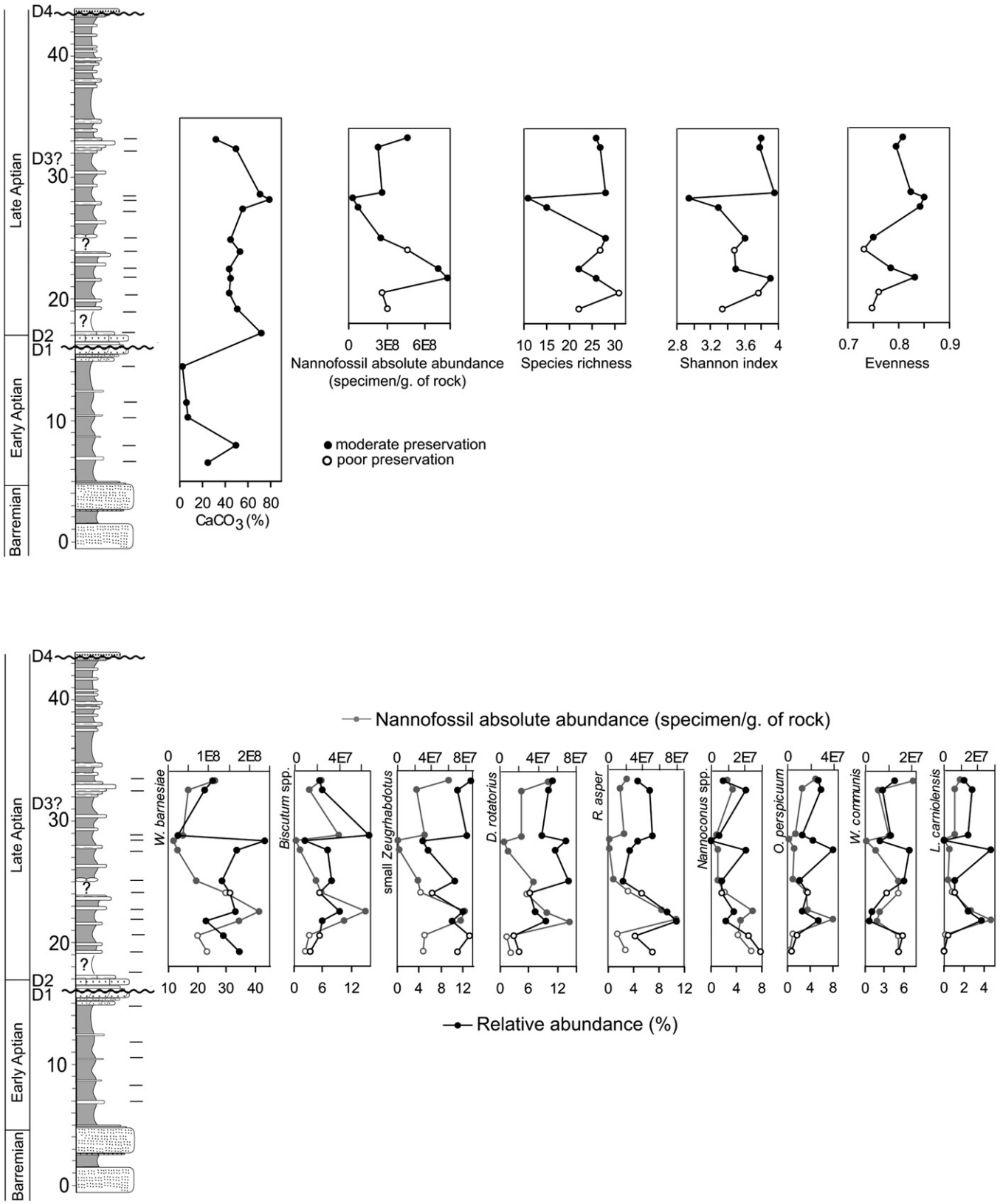

Fig. 5. Stratigraphic changes in calcium carbonate content, calcareous nannofossil total absolute abundance, species richness, diversity, evenness, and absolute and relative abundances of selected taxa for the Alma section. Position of samples is indicated by a small line.

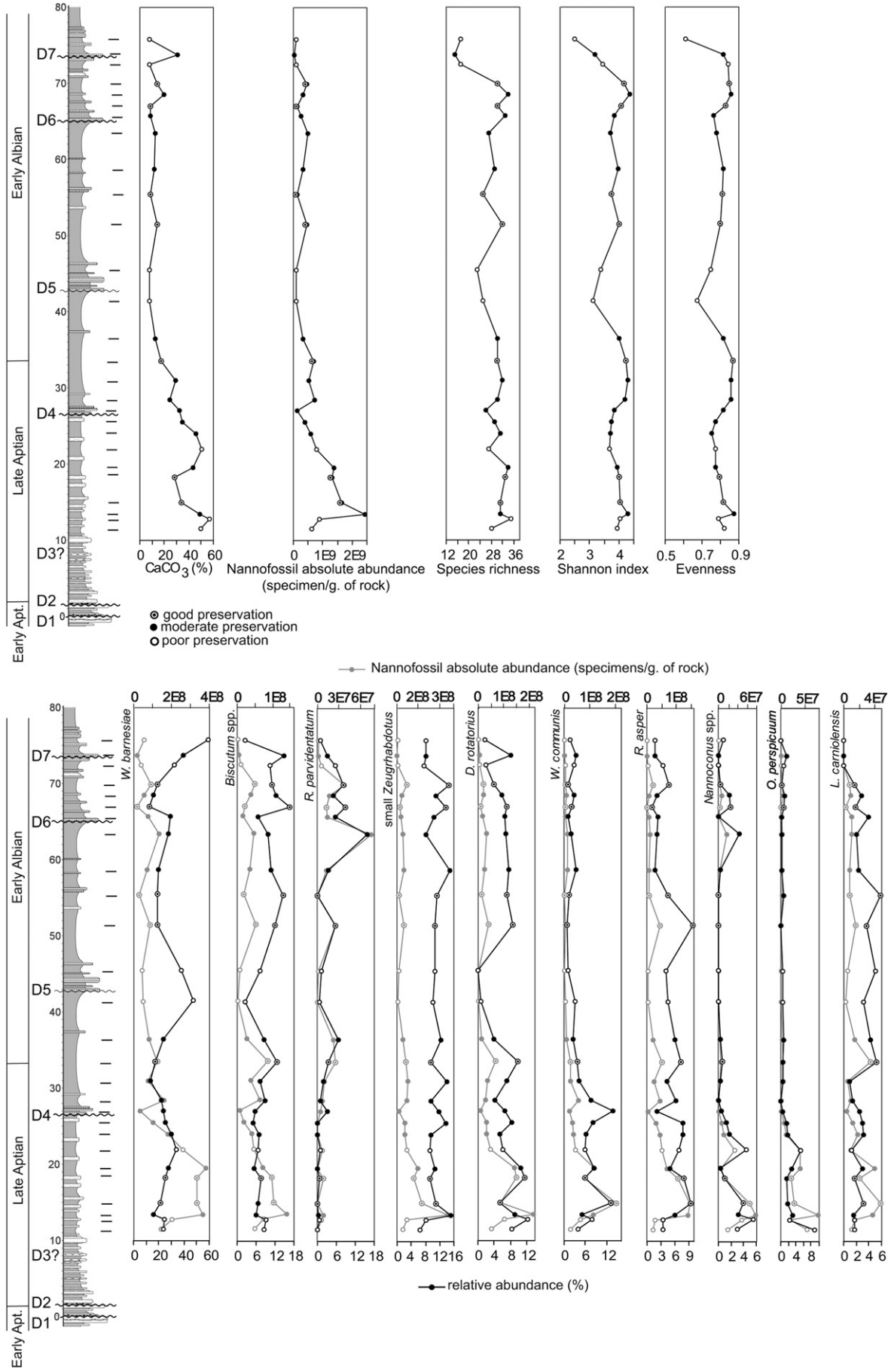

Fig. 6. Stratigraphic changes in calcium carbonate content, calcareous nannofossil total absolute abundance, species richness, diversity, evenness, and absolute, and relative abundances of selected taxa for the Addar section. Position of samples is indicated by a small line.

R. parvidentatum is synchronous to the decrease in both absolute and relative abundances of *R. asper*. *O. perspicuum* is well represented in the first 10 m of the succession whereas it becomes rare or absent at the top. *Nannoconus* spp. are usually present at the base and at the top of the succession, and *L. carniolensis* is more abundant in the middle part of the succession.

4.3.3. The Tamzergout section

With respect to the other sections, the Tamzergout section presents a dark color interval of approximately 8 m dated as Early Albian (Fig. 7). Below this interval, the calcium carbonate displays values between 20 and 37%. These values sharply decrease within the dark interval, and reach a minimum of 4.7%. Above this interval, the carbonate content increases.

Among the 19 selected samples, 3 are poorly preserved (categories E3/O2 or E2/O3) and are located in the dark interval, 11 samples are moderately preserved (categories E2 and O2) and 5 samples are well-preserved (categories E1 and O1). Well-preserved assemblages are mostly observed at the base of the section. The nannofossil absolute abundance ranges from 4.57×10^7 to 1.58×10^9 specimens per gram of sediment. The absolute abundances are higher in the lower part than in the upper part of the succession. The species richness varies from 16 to 38. The Shannon index and evenness fluctuate between 3.59–4.34, and 0.74–0.89, respectively. Nine species or group of species are well represented in the assemblages and display important abundance fluctuations; they are in decreasing order of abundance: *W. barnesiae* (av. v. of 24.5%, max. v. of 34.3%), *Biscutum* spp. (av. v. of 9.1%, max. v. of 14.3%), small *Zeugrhabdotus* (av. v. of 8.8%, max. v. of 14.8%), *W. communis* (av. v. of 6%, max. v. of 11.7%), *D. rotatorius* (av. v. of 5.4%, max. v. of 8.9%), *R. parvidentatum* (av. v. of 3.7%, max. v. of 8.2%), *R. asper* (av. v. of 3.1%, max. v. of 7.8%), *L. carniolensis* (av. v. of 1.9%, max. v. of 4.9%), and *O. perspicuum* (av. v. of 1.3%, max. v. of 3.3%). All taxa present a maximum in their absolute abundances at 57.5 m, which corresponds to a peak in the total absolute abundance. This level corresponds to a maximum flooding surface deduced from the sequence analysis of the section, and may, therefore, reflects a condensed level due to reduced sedimentation rate. The percentages of *R. asper* decrease from base to top of the section whereas those of *R. parvidentatum* generally present an opposite trend. This latter species presents the highest percentages within the dark interval, as does *W. communis*, of which the relative abundance is maximum at the base of the dark interval, and then sharply decreases until the top of this interval. The percentages of *L. carniolensis* decrease all along the succession, except in the dark levels where it increases. *O. perspicuum* is common in the lower part of the section until the base of the dark levels, and sharply decreases both in absolute and relative abundances above. *Nannoconus* are not represented in the Fig. 7, since their average percentages are generally below 1%.

5. Discussion

5.1. Calcareous nannofossil preservation

Three classes of nannofossil preservation have been identified in the sections of Alma, Addar and Tamzergout. Preservation state can control nannofossil abundance, species richness, and relative abundance of some species. Dissolution ranking of Cretaceous calcareous nannofossils has been proposed (Hill, 1975 (experimentation); Thierstein, 1980 (experimentation); Roth and Krumbach, 1986). Dissolution-resistant species are the large, thick placoliths with strongly imbricated elements (Hill, 1975) as *W. barnesiae*, which is considered the most resistant to dissolution (Hill, 1975; Thierstein, 1980, 1981; Roth, 1981; Roth and Bowdler, 1981; Roth and Krumbach, 1986). Thus, an increase of diagenetic alteration may imply an increase in the relative abundance of *W. barnesiae* and a concurrent decrease in the species richness of the assemblage. Conversely, *B. constans*, *Z. erectus*, *Discorhabdus*, are delicate taxa, considered to be very dissolution-susceptible forms (Hill, 1975; Thierstein, 1980; Roth, 1981; Roth and Bowdler, 1981; Roth and Krumbach, 1986), and an increase in diagenetic overprint may imply a decrease in their relative abundances. For all sections, we statistically tested the recognized effects of the different classes of preservation on nannofossil absolute abundance, species richness, relative abundances of *W. barnesiae* and of delicate taxa (*Biscutum* spp. + *D. rotatorius* + small *Zeugrhabdotus*; Fig. 8). Higher mean nannofossil absolute abundance, species richness, relative abundance of delicate taxa and lower mean percentages of *W. barnesiae* are recorded in samples presenting a good preservation (class E1-O1) with respect to the other classes (moderate preservation: E2-O2 and poor preservation: E3-O2/E2-O3). However, there are no statistically significant differences for means of these different parameters between the different classes of preservation (Fig. 8). We can therefore conclude that in the EAB, nannofossils are only moderately affected by diagenesis and may reflect original assemblage composition.

5.2. Carbonate production during the Late Aptian–Early Albian transition in the EAB

Considering the most complete section of Addar, the calcium carbonate content decreases progressively during the Late Aptian–Early Albian interval (Fig. 6). The variations of nannofossil absolute abundance follow those of the carbonate content (Fig. 6). The statistical correlation calculated between these two proxies from the entire dataset (49 samples from the three sections, except 2 poorly-preserved samples and some sterile samples; Table 2) displays a low positive correlation ($r = 0.318$, Table 2). This indicates that part of the carbonate fraction results from autochtonous carbonate production by nannofossils. Carbonate content is also positively correlated with the relative abundance of *Nannoconus* spp. (Table 2). *Nannoconus* are the biggest and more calcified nannofossils recognized within the assemblage, and are, therefore, the major component of the carbonate fraction produced by nannofossils.

Strong fluctuations of *Nannoconus* abundances are recorded during the Late Aptian–Early Albian both in the Tethyan and Pacific realms. The Late Aptian is characterized by high abundances of *N. truittii*, recognized as the "*Nannoconus truittii* Acme" described by Mutterlose (1989, 1991) and observed in the Tethyan and Boreal realms (Mutterlose, 1989; Erba, 1994; Herrle and Mutterlose, 2003). This acme occurs in the *martini* ammonite Zone. This time interval is present in the three studied sections of the EAB, but was only studied for nannofossils in the Alma section. The base of this section, characterized by the highest abundances of *Nannoconus* spp., mainly represented by *N. truittii*, could correspond to the end of this acme (Fig. 5). Latest Aptian and Early Albian times display a sharp decrease of *Nannoconus* abundances in the North Sea (Rückheim et al., 2006a, b), North Germany (Mutterlose et al., 2003), Italy (Erba, 1994; Cobianchi et al., 1997), the Vocontian Basin (Herrle and Mutterlose, 2003), and the Atlantic, Pacific and Antarctic oceans (Herrle, 2002; Wise, 1983; Mutterlose et al., 2009; Mutterlose and Wise, 1990). In the EAB, abundances of *Nannoconus* spp. sharply decrease during the latest Aptian (Alma and Addar sections; Figs. 5 and 6), and this species becomes rare during the Early Albian (Addar section; Fig. 6). Ecological affinities of *Nannoconus* spp. for warm and oligotrophic surface waters have been shown by numerous studies (Table 3). The decrease in both calcium carbonate content and *Nannoconus* abundances at the Aptian–Albian transition could

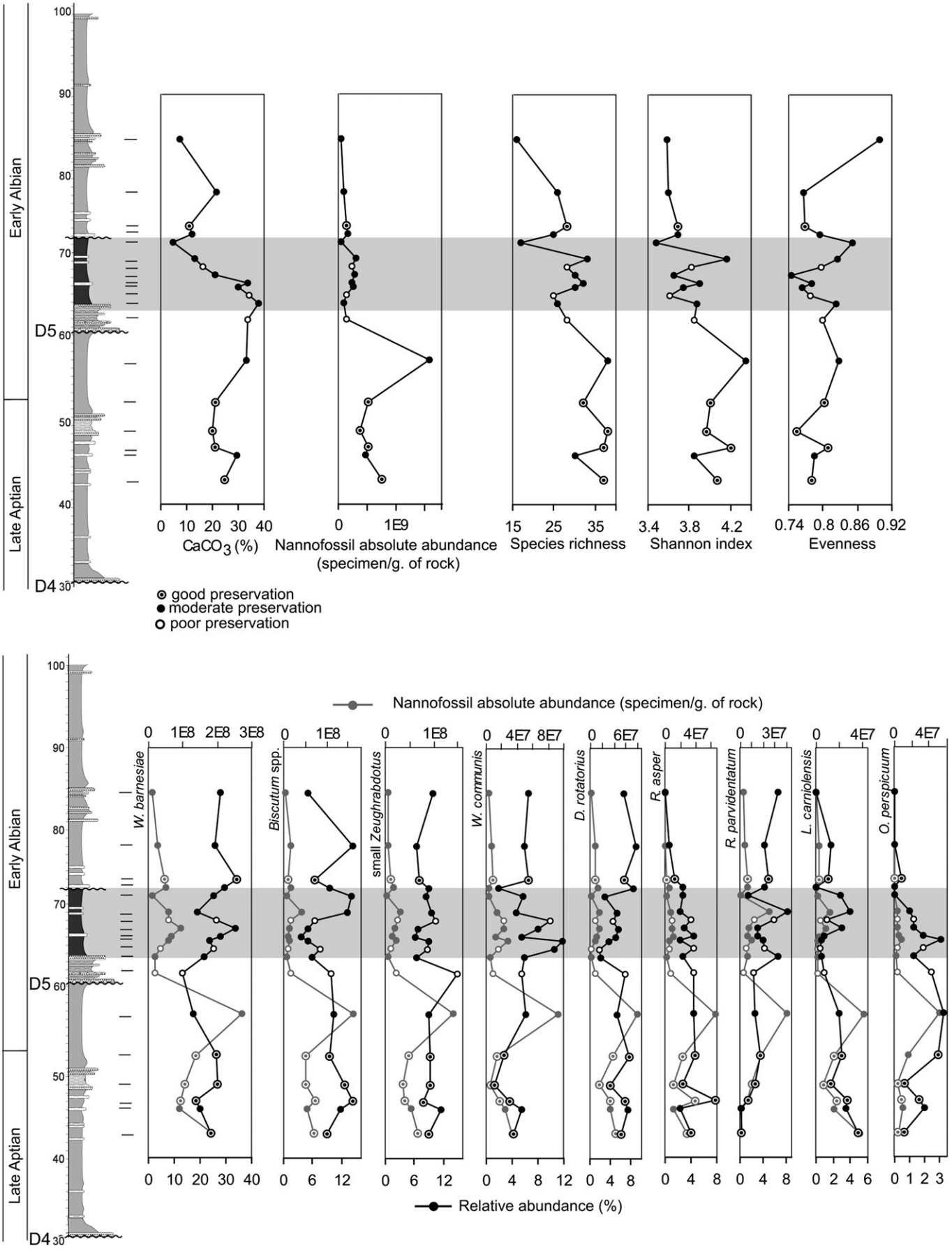

Fig. 7. Stratigraphic changes in calcium carbonate content, calcareous nannofossil total absolute abundance, species richness, diversity, evenness, and absolute and relative abundances of selected taxa for the Tamzergout section. Position of samples is indicated by a small line. The gray interval corresponds to dark levels recognized in this section.

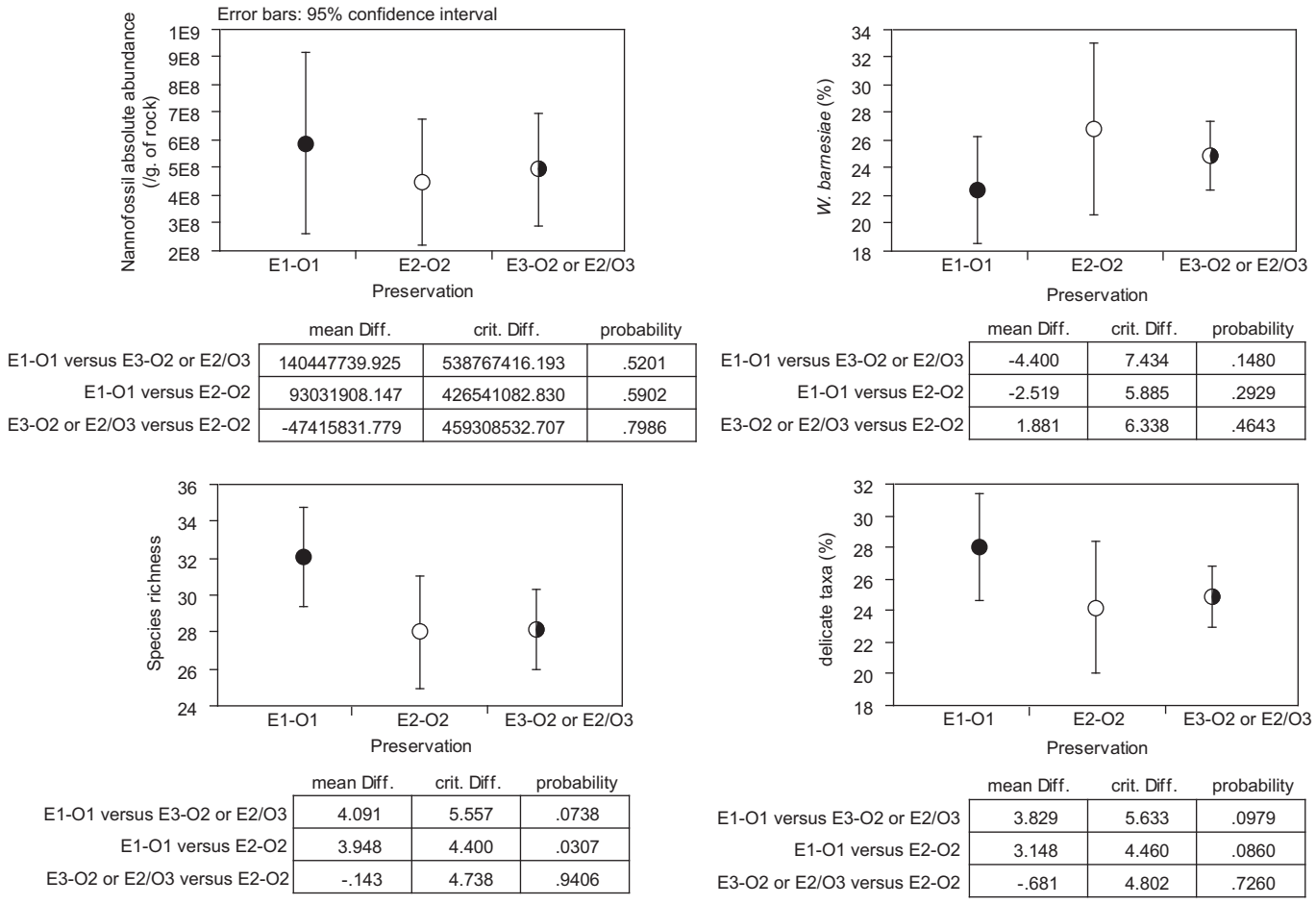

	mean Diff.	crit. Diff.	probability
E1-O1 versus E3-O2 or E2/O3	140447739.925	538767416.193	.5201
E1-O1 versus E2-O2	93031908.147	426541082.830	.5902
E3-O2 or E2/O3 versus E2-O2	-47415831.779	459308532.707	.7986

	mean Diff.	crit. Diff.	probability
E1-O1 versus E3-O2 or E2/O3	-4.400	7.434	.1480
E1-O1 versus E2-O2	-2.519	5.885	.2929
E3-O2 or E2/O3 versus E2-O2	1.881	6.338	.4643

	mean Diff.	crit. Diff.	probability
E1-O1 versus E3-O2 or E2/O3	4.091	5.557	.0738
E1-O1 versus E2-O2	3.948	4.400	.0307
E3-O2 or E2/O3 versus E2-O2	-.143	4.738	.9406

	mean Diff.	crit. Diff.	probability
E1-O1 versus E3-O2 or E2/O3	3.829	5.633	.0979
E1-O1 versus E2-O2	3.148	4.460	.0860
E3-O2 or E2/O3 versus E2-O2	-.681	4.802	.7260

Fig. 8. Mean nannofossil absolute abundance (specimens/gr. of rock), mean species richness, mean relative abundance of *W. barnesiae* and mean relative abundance of delicate taxa (*Biscutum* spp. + *D. rotatorius* + small *Zeugrhabdotus*) for different classes of preservation and for all the studied sections. In order to estimate the significance of the observed differences between the various classes of preservation, a Bonferroni/Dunn test is applied. It allows comparison of the calculated means for datasets with different sizes (here, the highly variable number of samples from one state of preservation to each other). Statistically significant differences were observed at p (probability) < 0.0167. Fifty-seven samples are considered in this analysis.

result from cooling climatic conditions and/or from associated increasing terrigenous input and nutrients, unfavorable to carbonate production. Mutterlose et al. (2009) suggest that the global cooling may have caused increased water circulation, leading to upwelling and increasing fertility of marine surface waters. However, in some places, as the south Atlantic margin, Late Aptian–Albian times correspond to a global "transgressive" period without significant terrigenous influx, and abundances of *Nannoconus* spp. remain low (B. Lambert, personal communication). After having dominated nannofossil assemblages in most Tethyan settings during the Lower Cretaceous (Busson and Noël, 1991; Street and Bown, 2000), the nannoconid population shows an abrupt decline "Nannoconid crisis" in the Early Aptian (Erba, 1994). A short-lived return marks the Late Aptian "*Nannoconus truittii* Acme" (Mutterlose, 1989, 1991) that did not reach the former abundance, and is followed by a new drastic decrease of *Nannoconus* abundance in the middle Late Aptian (nannoconid crisis II; Herrle and Mutterlose, 2003). Locally, *Nannoconus* can be significant contributors in some upper cretaceous chalks (as for instance, the Turonian of the Paris basin, Aubry, 1970), but at a global scale, they are rare after the upper Aptian times, and became extinct in the Late Campanian (Burnett et al. in Bown et al., 1998).

So the reduction of nannoconids observed at the end of the Aptian could be the result of cooling at low latitudes, but the major decline is observed before with the two Aptian nannoconid crises, which seem synchronous with major drowning events of carbonate

Table 2
Correlation analyses between calcium carbonate content, nannofossil absolute abundance (specimens/gr. of rock), species richness, diversity and evenness, and the relative abundance of *Nannoconus* spp. The number of measurements is 49. The Correlation coefficient of Pearson is in bold where it is statistically significant (p (probability) < 0.05).

	$CaCO_3$ (%)	Nannof. abs. ab. (sp./g of rock)	Species richness	Shannon index	Evenness	*Nannoconus* spp. (%)
$CaCO_3$ (%)	1.000					
Nannof. abs. ab. (sp./g of rock)	**0.318**	1.000				
Species richness	−0.124	**0.479**	1.000			
Shannon index	−0.157	**0.484**	**0.717**	1.000		
Evenness	−0.116	0.285	0.170	**0.807**	1.000	
Nannoconus spp. (%)	**0.652**	0.241	−0.213	−0.203	−0.108	1.000

Table 3
Paleoecological significance of selected nannofossil taxa.

Taxa	Fertility of surface waters	Paleoceanography
B. constans	eutrophic[1, 2, 3, 4, 5, 6, 7, 8]	
B. ellipticum[a]	eutrophic[2]	
	meso-eutrophic[9]	
Biscutum spp.[b]	mesotrophic[10]	
D. rotatorius	meso-eutrophic[4, 9, 11, 12, 13]	
L. carniolensis	mesotrophic[4, 11]	
Z. erectus	eutrophic[2, 3, 4, 5, 7, 8, 13]	
small *Zeugrhabdotus* (major axis $\leq$ 5 μm)	eutrophic[3, 14]	
Nannoconus spp.	oligotrophic[8, 12, 17]	warm waters[8, 15, 16]
R. asper		warm waters[4, 11, 14, 15, 18]
R. parvidentatum		high latitude[14, 18, 19]

[1]Roth, 1981; [2]Roth and Bowdler 1981; [3]Roth and Krumbach, 1986; [4]Premoli Silvá et al., 1989; [5]Roth, 1989; [6]Watkins 1989; [7]Williams and Bralower 1995; [8]Mutterlose and Kessels 2000; [9]Giraud et al., 2003; [10]Linnert et al., 2010; [11]Erba, 1992; [12]Coccioni et al., 1992; [13]Herrle et al., 2003; [14]Erba et al., 1992; [15]Mutterlose, 1989; [16]Street and Bown 2000; [17]Erba, 1994; [18]Crux, 1991; [19]Wise, 1988.

[a] *B. ellipticum* is considered as a morphotype of *B. constans* (Bornemann and Mutterlose, 2006).

[b] *Biscutum* spp.: *B. constans* (abundant), *B. ellipticum* (common) (Linnert et al., 2010).

platforms, possibly reflecting a collapse in the marine carbonate system on a global scale (Herrle and Hemleben, 2001).

5.3. Climatic conditions during the Late Aptian–Early Albian transition in the EAB

The Aptian–Albian transition has been identified as a period of substantial climate cooling. Evidences for this cooling episode mainly proceed from high-latitude records and are supported by lithological, geochemical and paleontological proxies (see Heimhofer et al. (2008) for a synthesis). Decreasing surface water temperatures are indicated by a first global decline of Tethyan nannoconids in the Late Aptian at both high and low latitudes, associated with increasing nannofossil boreal taxa in low latitudes during the latest Aptian to earliest Albian period (Herrle and Mutterlose, 2003; Mutterlose et al., 2009).

If we consider nannofossil taxa as indicators of changes in sea surface temperatures in the EAB, strong variations in both the absolute and the relative abundances of three taxa must be taken into account: *Nannoconus* spp. (already described in the preceeding section), *R. parvidentatum* and *R. asper*. *R. parvidentatum* is a high-latitude species (Table 3). Its occurrence in the Tethyan realm during the Early Albian evidences communications with the Boreal realm (Herrle and Mutterlose, 2003). Such communications could be favored by a higher sea level during the Early Albian compared to the Aptian times (Haq et al., 1987). However, taxa with Tethyan affinities, like *R. asper,* indicative of warmer sea surface temperature (Table 3) decreased in the North Sea and North Germany during the Early Albian (Jeremiah, 1996, 2001; Rückheim et al., 2006a, b), as did Tethyan nannoconids.

R. parvidentatum is absent (Alma section; Fig. 5) or rare (Addar and Tamzergout sections; Figs. 6 and 7) during the Late Aptian, whereas it increases both in absolute and relative abundances during the Early Albian (Addar and Tamzergout sections; Figs. 6 and 7). These results evidence a decrease of sea surface temperature in the EAB at that time, allowing migration of nannoflora from high to low latitudes. The decrease in absolute and relative abundances of *R. asper* during the same time interval for the three sections (Figs. 5–7) supports this interpretation.

Our study shows, therefore, that the cooling episode identified elsewhere at the Aptian–Albian transition, is recognized in the EAB.

5.4. Nannofossil productivity during the Late Aptian–Early Albian transition in the EAB (Addar and Tamzergout sections)

Variations in nannofossil productivity are estimated in the EAB taking into account and comparing two proxies: the relative abundance of meso-eutrophic nannofossil taxa recognized in our samples (*Biscutum* spp., *D. rotatorius*, small *Zeugrhabdotus* and *L. carniolensis*; their paleoecology are summarized in Table 3), and the nannofossil fluxes calculated for some well-calibrated time interval using the results of Herrle (2002). Only the Addar and Tamzergout sections, in which the same time interval has been studied for nannofossils, are considered for the calculation of fluxes and estimation of productivity.

The relative abundances of the meso-eutrophic taxa do not present strong fluctuations in the Addar section, whereas in the Tamzergout section, where dark levels are recognized, stronger variations in percentages are observed (Fig. 9). The abundances of meso-eutrophic taxa sharply decrease at the base of the dark levels, and then progressively increase in the upper part of the darker interval to reach values similar to those found in the rest of the section.

On the basis of biostratigraphic and chemostratigraphic results, Herrle (2002) proposed a correlation between the Niveau Paquier recognized in the Vocontian Basin and the OAE 1b identified on the Mazagan Plateau. The Niveau Paquier, and the dark levels of the EAB are both dated from the *tardefurcata* ammonite Zone, and can be considered synchronous. Therefore, although sedimentological and geochemical studies have not been carried out, it could be possible that the dark interval, only recognized in the median part of the EAB, represent the lithological expression of the OAE 1b.

Based on mean sedimentation rates calculated with biostratigraphic and cyclostratigraphic time control by Herrle (2002), the estimated duration of the *tardefurcata* ammonite Zone is 1.08 my (Table 4).

Although the *tardefurcata* ammonite Zone time interval is only represented by 5 samples in the Addar section, the nannofossil fluxes seem to be higher in Tamzergout than in Addar (Fig. 9). In the Tamzergout section, the nannofossil flux sharply decreases just before deposition of the dark levels. Considering both the relative abundance of meso-eutrophic taxa and flux in the Tamzergout section, the nannofossil productivity is higher below the dark interval than within it. For the time interval corresponding to the *tardefurcata* Zone, the mean relative abundance of meso-eutrophic taxa is similar in the Addar and Tamzergout sections, whereas the mean nannofossil flux is higher in Tamzergout than in Addar (Table 4). So there are some discrepancies between results obtained from meso-eutrophic taxa percentages and fluxes. The results obtained from fluxes suggest that the nannofossil productivity is higher in Tamzergout than in Addar. This can be explained by the fact that since Tamzergout is located in a more proximal position with respect to Addar, more nutrients associated to runoff are expected to be available in more proximal environments.

5.5. Comparison of nannofossil productivity between the southern and northern Tethyan margins

In this section, we compare the mean nannofossil productivity between the southern Tethyan margin (EAB and Mazagan Plateau) and northern Tethyan margin (Vocontian Basin), using the data by Herrle (2002). For this comparison, we choosed two proxies available for all settings, the relative abundance of meso-eutrophic taxa, and the nannofossil fluxes.

The comparison of nannofossil fluxes is possible since in the work by Herrle (2002) and in the present study, the same

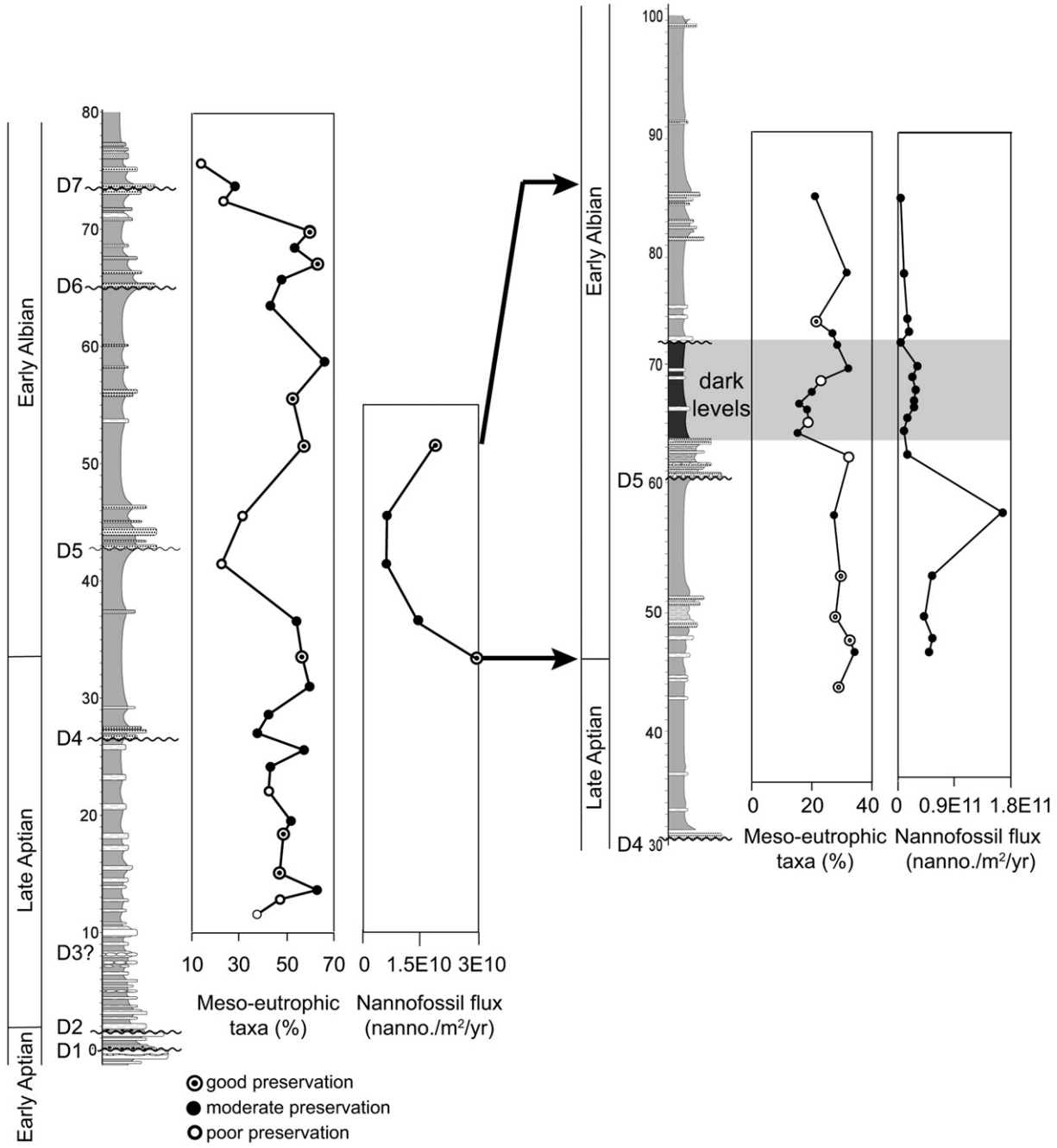

Fig. 9. Stratigraphic changes in meso-eutrophic taxa (*Biscutum* spp. + *D. rotatorius* + *L. carniolensis* + small *Zeugrhabdotus*) percentages and nannofossil fluxes for the Addar and Tamzergout sections.

random settling method of Geisen et al. (1999) was performed to prepare nannofossil smear slides and to calculate absolute abundance.

The mean nannofossil productivity was compared for the time interval corresponding to the *tardefurcata* Zone (Early Albian), which is recovered for the EAB (Addar and Tamzergout sections), the Mazagan Plateau and the Vocontian Basin.

During the Early Albian, the mean relative abundance of the meso-eutrophic taxa was higher on the Mazagan Plateau than in the Vocontian Basin and in the EAB (Fig. 10). The Mazagan Plateau

Table 4
Mean percentages of meso-eutrophic taxa (*Biscutum* spp. + *D. rotatorius* + *L. carniolensis* + small *Zeugrhabdotus*), nannofossil absolute abundances and fluxes in the Addar and Tamzergout sections for the time interval corresponding to the *tardefurcata* ammonite Zone. The thickness of this zone is given for each section. The duration of the *tardefurcata* Zone is estimated from results of Herrle (2002), allowing calculation of sedimentation rates for the two sections.

	Meso-eutrophic taxa (%)	Nannofossil absolute abundance	Thickness of the *tardefurcata* Zone (m)	Duration of the *tardefurcata* Zone (my)	Sedimentation rate (cm/ky)	Nannofossil flux (nanno./m^2/yr)
Addar	23.9	3.36E+08	19	1.08	1.76	1.6E+10
Tamzergout	23.6	3.47E+08	41	1.08	3.9	3.66E+10

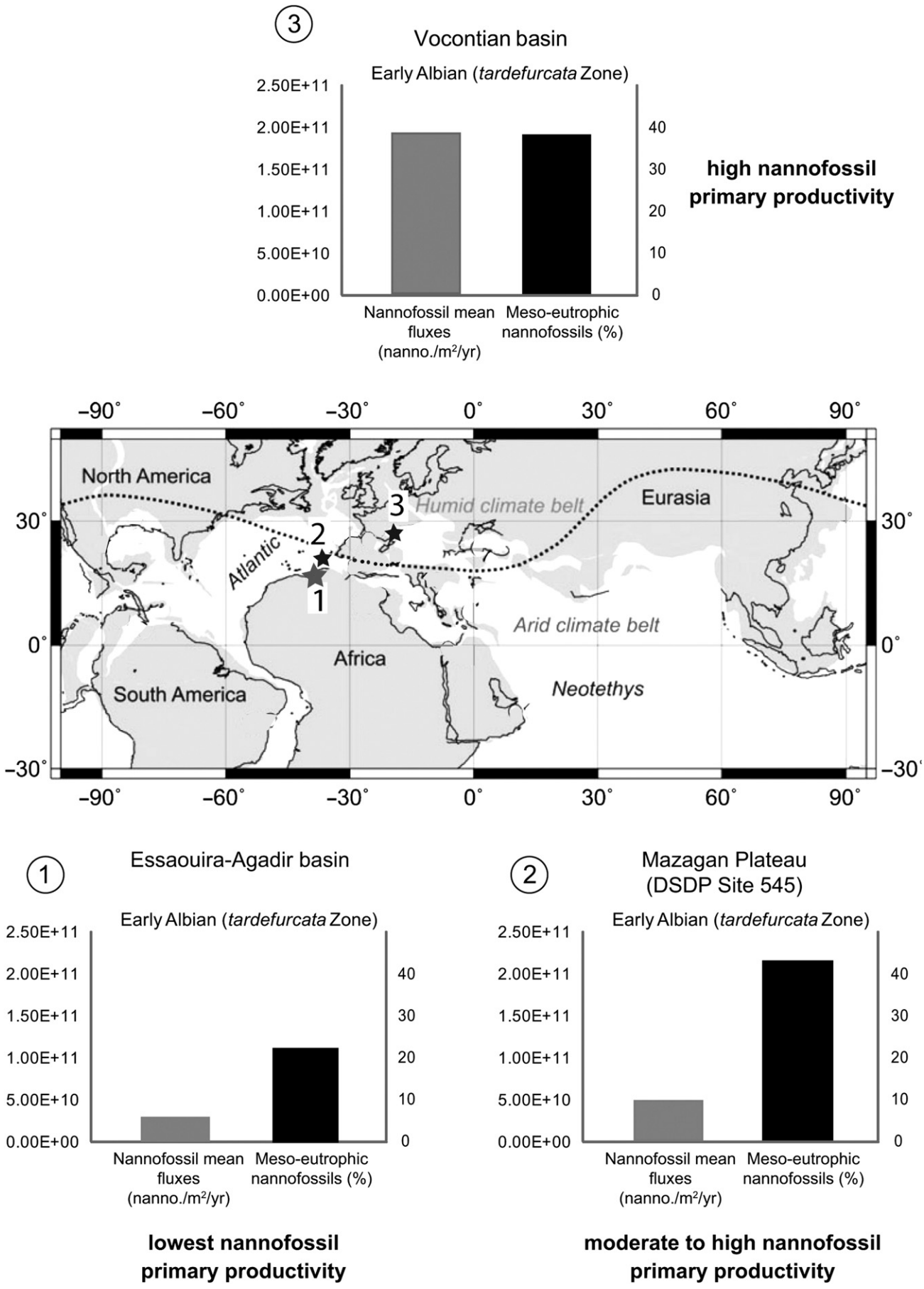

Fig. 10. Mean nannofossil fluxes and mean meso-eutrophic taxa percentages for the Agadir basin, the Mazagan Plateau (DSDP Site 545) and the Vocontian Basin for the earliest Albian (*tardefurcata* ammonite Zone). For the Vocontian Basin and the Mazagan Plateau, data are compiled from Herrle (2002). The Late Aptian paleogeographic map is modified from Heldt et al. (2010).

was submitted to upwelling conditions during this period. The presence of upwelling was suggested by Leckie (1984), based on the high abundance of radiolarians, the high benthic/planktonic foraminifera ratio and the high abundance of fish debris.

However, results obtained from the mean nannofossil fluxes data do not correlate with the relative abundances of meso-eutrophic taxa. The Vocontian Basin is characterized by nannofossil fluxes four times higher than those of the Mazagan Plateau, and height times higher than those of the EAB (Fig. 10). On the southern Tethyan margin, the nannofossil productivity is lower in the EAB than on the Mazagan Plateau. This indicates that our study area of the EAB was located outside the main upwelling area, without excluding totally the presence of upwelling in the EAB.

Our data show that the estimates of the nannofossil productivity are different, depending on the proxies we used. How can we explain these differences? As already discussed by Williams and Bralower (1995), the relative abundances data are affected by "closed-sum" problems and the high relative abundance of one species can be interpreted as a real increase in abundance of this species, or as a decrease in abundance of the other species. Considering the nannofossil fluxes, the comparison between the southern and the northern Tethyan margins shows that the nannofossil productivity is higher in the Vocontian Basin with respect to both the Mazagan Plateau and the EAB during the Late Aptian–Early Albian interval. The Vocontian Basin is located in the humid climatic belt of Chumakov et al. (1995) (Fig. 10), and more nutrients are associated to runoff. Moreover, Herrle (2002) and Herrle et al. (2003) showed that the Vocontian Basin was submitted to a monsoon climate-type during the Early Albian.

However, the clay mineral assemblages from different low to mid palaeolatitudes, including the Algarve basin (Heimhofer et al., 2008), the EAB (SW Morocco; Daoudi and Deconinck, 1994) and the Vocontian Basin (SE France; Bréhéret, 1997), show very similar patterns with high abundances of illite, indicating high physical weathering rates. This is in agreement with an arid climate in both the northern and southern margins of the Tethys.

Consequently, trophic conditions in sea surface were probably lower, both in neritic (results of Heldt et al., 2010) and pelagic realms on the southern Tethyan margin, with respect to the northern margin, likely due to more arid climatic conditions to the South.

6. Conclusions

A high resolution ammonite biostratigraphy and recognition of major sedimentary unconformities allowed good correlation of five sections located on a proximal (Tinfoul section) – distal (Tamri section) transect in the EAB encompassing the Aptian–Early Albian interval. Dark levels are recognized in the Tamzergout section; they are dated from the *tardefurcata* ammonite Zone and could be synchronous with the black shales of the Niveau Paquier in the Vocontian Basin, a lithological expression of the OAE 1b.

A decrease in carbonate productivity, is revealed by the calcium carbonate content and nannofossils abundances, at the Aptian–Albian transition. It could result from cooler climatic conditions recognized in the EAB, as well as in other basins, and/or from the associated increasing terrigenous input and nutrients, which hindered carbonate production. In the EAB, the nannofossil productivity is higher before deposition of the dark levels, in the earliest Albian.

The nannofossil productivity in two sites of the southern Tethyan margin (EAB, this study; DSDP site 545, Mazagan Plateau submitted to upwelling conditions, Herrle, 2002) and one site of the northern Tethyan margin (Vocontian Basin, Herrle, 2002) has been compared. This comparison shows that the nannofossil fluxes and percentages of meso-eutrophic taxa are not correlated.

During the Early Albian, the Vocontian Basin is characterized by nannofossil fluxes four times higher than those of the upwelling-submitted Mazagan Plateau, and height times higher than those of the EAB. Conversely, the meso-eutrophic taxa are slightly more abundant on the Mazagan Plateau than in the Vocontian Basin.

These data seem to corroborate the results of Heldt et al. (2010) and show that trophic conditions in sea surface waters were lower not only in the neritic, but also in the pelagic realm of the southern Tethyan margin with respect to the northern margin, probably due to more arid climatic conditions on the southern Tethyan margin.

Acknowledgments

This work is a contribution to the team project 'Tectonic, Relief, Basin' of the CNRS-UMR 5275 ISTerre, Grenoble. We thank the Laboratoire de géologie de Lyon: Terre, Planètes, Environnement, and the Institut de Recherche pour le Développement (IRD) for financial support. Thoughtful suggestions of Bernard Lambert, of two other anonymous reviewers and of Peter Skelton (managing guest editor) helped to improve the manuscript.

References

Algouti, A., Algouti, A., Taj-Eddine, K., 1999. Le Sénonien du Haut Atlas occidental, Maroc: sédimentologie, analyse séquentielle et paléogéographie. Journal of African Earth Sciences 29, 643–658.

Ambroggi, R., 1963. Etude géologique du versant méridional du Haut Atlas occidental et de la plaine du Souss. Notes du Service géologique du Maroc 157, 322.

Ando, A., Kaiho, K., Kawahata, H., Hakegawa, T., 2008. Timing and magnitude of early Aptian extreme warming: unraveling primary $\delta^{18}O$ variation in indurated pelagic carbonates at Deep Sea Drilling Project Site 463, central Pacific Ocean. Palaeogeography, Palaeoclimatology, Palaeoecology 260, 463–476.

Andreu, B., 1989. Le Crétacé moyen de la transversale Agadir-Nador (Maroc): précisions stratigraphiques et sédimentologiques. Cretaceous Research 10, 49–80.

Andreu, B., 1992. Distribution stratigraphique des ostracodes du Barrémien au Turonien, le long d'une transversale Agadir-Nador (Maroc). Géologie Méditerranéenne 19, 165–187.

Arthur, M.A., Jenkyns, H.C., Brumsack, H.J., Schlanger, S.O., 1990. Stratigraphy, geochemistry and paleoceanography of organic carbon-rich Cretaceous sequences. In: Ginsburg, R.N., Beaudoin, B. (Eds.), Cretaceous Resources, Events and Rhythms. NATO ASI Series C: Springer-Verlag, Berlin, 304, pp. 75–119.

Aubry, M.-P., 1970. Importance géologique des Nannoconus dans les craies turoniennes de la région dieppoise. Bulletin de la Société Géologique de Normandie LX, 1–8.

Aubry, M.-P., Bord, D., Beaufort, L., Kahn, A., Boyd, S., 2005. Trends in size changes in the coccolithophorids, calcareous nannoplankton, during the Mesozoic: a pilot study. Micropaleontology 51, 309–318.

Beaufort, L., 1991. Adaptation of the random settling method for quantitative studies of calcareous nannofossils. Micropaleontology 37, 415–418.

Bornemann, A., Aschwer, U., Mutterlose, J., 2003. The impact of calcareous nannofossils on the pelagic carbonate accumulation across the Jurassic-Cretaceous boundary. Palaeogeography, Palaeoclimatology, Palaeoecology 199, 187–228.

Bornemann, A., Pross, J., Reichelt, K., Herrle, J.O., Hemleben, C., Mutterlose, J., 2005. Reconstruction of short-term palaeoceanographic changes during the formation of the Late Albian 'Niveau Breitroffer' black shales (Oceanic Anoxic Event 1d, SE France). Journal of the Geological Society of London 162, 101–114.

Bornemann, A., Mutterlose, J., 2006. Size analyses of the coccolith species *Biscutum constans* and *Watznaueria barnesiae* from the Late Albian "Niveau Breistroffer" (SE France): taxonomic and palaeoecological implications. Geobios 39, 599–615.

Bouatmani, R., Chakor Alimi, A., Medina, F., 2007. Subsidence, évolution thermique et maturation des hydrocarbures dans le bassin d'Essaouira (Maroc): apport de la modélisation. Bulletin de l'Institut Scientifique Rabat 29, 15–36.

Bourgeoini, Y., 1994. Etude micropaléontologique et biostratigraphique de l'Aptien et de l'Albien du bassin d'Essaouira. Haut Atlas occidental. Maroc. Mémoire de doctorat de l'Université de Tunis. 274 pp.

Bourgeoini, Y., Ben Haj Ali, N., Razgallah, S., Tajeddine, K., 2002. Etude biostratigraphique du Crétacé inférieur (Barrémien supérieur-Albien) du Haut Atlas occidental (Maroc). Estudios Geologicos 58, 105–112.

Bralower, T.J., Sliter, W.V., Arthur, M.A., Leckie, R.M., Allard, D., Schlanger, S.O., 1993. Dysoxic/anoxic episodes in the Aptian-Albian (Early Cretaceous). In: Pringle, M.S., Sager, W.W., Sliter, W.V., Stein, S. (Eds.), The Mesozoic Pacific: Geology, Tectonics, and Volcanism. Am. Geophys. Union Geophys. Monogr. 77, pp. 5–37.

Bralower, T.J., Arthur, M.A., Leckie, R.M., Sliter, W.V., Allard, D.J., Schlanger, S.O., 1994. Timing and paleoceanography of oceanic dysoxia/anoxia in the late Barremian to early Aptian (Early Cretaceous). Palaios 9, 335–369.

Bréhéret, J.-G., 1997. L'Aptien et l'Albien de la fosse vocontienne (bordures au bassin): Evolution de la sédimentation et enseignements sur les événements anoxiques. Publication de la Société Géologique du Nord 25, 1–614.

Brives, A., 1905. Contribution à l'étude géologique de l'Atlas marocain. Bulletin de la Société géologique de France 5, 379–398.

Broughton, P., Trépanier, A., 1993. Hydrocarbon generation in the Essaouira Basin of western Morocco. American Association of Petrologist and Geologist Bulletin 77, 999–1015.

Burnett, J.A., Gallagher, L.T., Hampton, M.J., 1998. Upper Cretaceous. In: Bown, P.R. (Ed.), Calcareous nannofossil biostratigraphy. British Micropalaeontological Society Publications Series. Chapman and Hall/Kluwer Academic Publishers, pp. 132–199.

Busson, G., Noël, D., 1991. Les Nannoconidés, indicateurs environnementaux des océans et mer épicontinentales du Jurassique terminal et du Crétacé inférieur. Oceanologica Acta 14, 333–356.

Butt, A., 1982. Micropaleontological bathymetry of cretaceous of western Morocco. Palaeogeography, Palaeoclimatology, Palaeoecology 37, 235–275.

Canérot, J., Cugny, P., Peybernès, B., Rahli, I., Rey, J., Thieuloy, J.-P., 1986. Comparative study of the Lower and Mid-Cretaceous sequences on different maghrebian shelves and basins: Their place in the evolution of the North African, Atlantic and Neotethysian margins. Palaeogeography, Palaeoclimatology, Palaeoecology 55, 213–232.

Chumakov, N.M., Zharkov, M.A., Herman, A.B., Doludenko, M.P., Kalandadze, N.M., Lebedev, E.L., Ponomareko, A.G., Rautian, A.S., 1995. Climatic belts of the mid-Cretaceous time. Stratigraphy and Geological Correlation 3, 241–260.

Cobianchi, M., Luciani, V., Bosellini, A., 1997. Early Cretaceous nannofossils and planktonic foraminifera from northern Gargano (Apulia, southern Italy). Cretaceous Research 18, 249–293.

Coccioni, R., Premoli Silvá, I., Erba, E., 1992. Barremian-Aptian calcareous plankton biostratigraphy from the Gorgo Cerbara section (Marche, central Italy) and implications for plankton evolution. Cretaceous Research 13, 517–537.

Company, M., Saandoval, J., Tavera, J.M., Aoutem, M., Ettachfini, M., 2008. Barremian ammonite faunas from the western High Atlas, Morocco – biostratigraphy and palaeobiogeography. Cretaceous Research 29, 9–26.

Coward, M.P., Ries, A.C., 2003. Tectonic development of North African basins. In: Arthur, T.J., MacGregor, D.S., Cameron, N.R. (Eds.), Petroleum Geology of Africa: New themes and developing technologies. The Geological Society of London, Special Publication 207, pp. 61–83.

Crux, J.A., 1991. Albian calcareous nannofossils from the Gault Clay of Munday's Hill (Bedfordshire, England). Journal of Micropaleontology 10, 203–222.

Daoudi, L., Deconinck, J.-F., 1994. Contrôles paléogéographique et diagénétique des successions sédimentaires argileuses du Bassin Atlasique au Crétacé (Haut-Atlas Occidental, Maroc). Journal of African Earth Sciences 18, 123–141.

Davison, I., 2005. Central Atlantic margin basins of North West Africa: Geology and hydrocarbon potential (Morocco to Guinea). Journal of African Earth Sciences 43, 254–274.

Davison, I., Davy, P., 2010. Salt tectonics in the Cap Boudjour Area, Aaiun basin, NW Africa. Marine and Petroleum Geology 27, 435–441.

Dubourdieu, G., 1953. Ammonites nouvelles des Monts du Mellègue. In: Dubourdieu, G. (Ed.), 1953. Bulletin du Service de la Carte Géologique d'Algérie. 1ère série. Paléontologie 16, pp. 1–76.

Duffaud, F., Brun, L., Plauchut, B., 1966. Le bassin du Sud-Ouest marocain. In: Reyre, D. (Ed.), Bassins sédimentaires du Littoral africain, 1ère partie. Frimin Didot Publications, Paris, pp. 5–12.

Erba, E., 1992. Calcareous nannofossil distribution in pelagic rhythmic sediments (Aptian Albian Piobbico core, central Italy). Rivista Italiana Paleontologia Stratigraphica 97, 455–484.

Erba, E., 1994. Nannofossils and superplumes: the early Aptian "nannoconid crisis". Paleoceanography 9, 483–501.

Erba, E., Castradori, D., Guasti, G., Ripepe, M., 1992. Calcareous nannofossils and Milankovitch cycles: the example of the Albian Gault Clay Formation (southern England). Palaeogeography, Palaeoclimatology, Palaeoecology 93, 47–69.

Essafraoui, B., Grosheny, D., Içame, N., Masrour, M., Aoutem, M., Bulot, L., Lecuyer, C., 2010. The fluvial-marine transition in genetic sequences of the uppermost Albian («Vraconian») of the Moroccan Atlantic margin (Agadir area). In: Grosheny, D., Granier, B., Sander, N. (Eds.), Platform to basin correlations in Cretaceous times, p. 6.

Ettachfini, E.M., Andreu, B., 2004. Le Cénomanien et le Turonien de la plate-forme Préafricaine du Maroc. Cretaceous Research 25, 277–302.

Ettachfini, E.M., Souhlel, A., Andreu, B., Caron, M., 2005. La limite Cénomanien-Turonien dans le Haut Atlas central, Maroc. Geobios 38, 57–68.

Fisher, R.A., 1921. On the 'probable error' of a coefficient of correlation deduced from a small sample. Metron 1, 3–32.

Föllmi, K.B., Godet, A., Bodin, S., Linder, P., 2006. Interactions between environmental change and shallow water carbonate buildup along the northern Tethyan margin and their impact on the Early Cretaceous carbon isotope record. Paleoceanography 21 (PA4211), 1–16.

Frakes, L.A., Francis, J.E., 1988. A guide to Phanerozoic cold polar climates from high-latitude ice-rafting in the Cretaceous. Nature 333, 547–549.

Frizon de la Motte, D., Saint Bezar, B., Bracène, R., 2000. The two main steps of the Atlas building and geodynamics of the western Mediterranean. Tectonics 19, 740–761.

Frizon de la Motte, D., Zizi, M., Missenard, Y., Hafid, M., El Azzouzi, M., Maury, R.C., Charrière, A., Taki, Z., Benammi, M., Micard, A., 2008. The Atlas System. In: Michard, A., et al. (Eds.), Continental Evolution: The Geology of Morocco. Lecture Notes in Earth Sciences 116, pp. 133–202.

Geisen, M., Bollmann, J., Herrle, J.O., Mutterlose, J., Young, J.R., 1999. Calibration of the random settling technique for calculation of absolute abundances of calcareous nannoplankton. Micropaleontology 45, 437–442.

Gentil, L., 1905. Observations géologiques dans le sud marocain. Bulletin de la Société géologique de France 5, 521–523.

Giraud, F., Olivero, D., Baudin, F., Reboulet, S., Pittet, B., Proux, O., 2003. Minor changes in surface water fertility across the Oceanic Anoxic Event 1d (latest Albian, SE France) evidenced by calcareous nannofossils. International Journal of Earth Sciences 92, 267–284.

Hafid, M., 2000. Triassic-Liassic extensional systems and their Tertiary inversion, Essaouiara Basin (Morocco). Marine and Petroleum Geology 17, 409–429.

Hafid, M., Aït Salem, A., Bally, A.W., 2000. The western termination of the Jebilet-High Atlas system (offshore Essaouiara Basin, Morocco). Marine and Petroleum Geology 17, 431–443.

Hafid, M., Tari, G., Bouhadioui, D., El Moussaid, I., Aït Salem, A., Nahim, M., Dakki, M., 2008. Atlantic Basins. In: Michard, A., et al. (Eds.), Continental Evolution: the Geology of Morocco. Lecture Notes in Earth Sciences 116, pp. 303–329.

Hallock, P., Schlager, W., 1986. Nutrient Excess and the Demise of Coral reefs and Carbonate Platforms. Palaios 1, 389–398.

Haq, B.U., Hardenbol, J., Vail, P.R., 1987. Chronology of fluctuating sea-levels since the Triassic. Science 235, 1156–1167.

Hardas, P., Mutterlose, J., 2007. Calcareous nannofossil assemblages of Oceanic Anoxic Event 2 in the equatorial Atlantic: evidence of an eutrophication event. Marine Micropaleontology 66, 52–69.

Heimhofer, U., Adatte, T., Hochuli, P.A., Burla, S., Weissert, H., 2008. Coastal sediments from the Algarve: low-latitude climate archive for the Aptian-Albian. International Journal of Earth Sciences 97, 785–797.

Heldt, M., Bachmann, M., Lehmann, J., 2008. Microfacies, biostratigraphy, and geochemistry of the hemipelagic Barremian–Aptian: influence of the OAE 1a on the southern Tethys margin. Palaeogeography, Palaeoclimatology, Palaeoecology 261, 246–260.

Heldt, M., Lehmann, J., Bachmann, M., Negra, H., Kuss, J., 2010. Increased terrigenous influx but no drowning: palaeoenvironmental evolution of the Tunisian carbonate platform margin during the Late Aptian. Sedimentology 57, 695–719.

Herrle, J.O., 2002. Mid-Cretaceous paleoceanographic and paleoclimatologic implications on black shale formation of the Vocontian Basin and Atlantic. Evidence from calcareous nannofossils and stable isotopes. Tübinger Mikropaläontologische Mitteilungen 27, 114.

Herrle, J.O., Hemleben, C., 2001. Positive carbon isotope excursions of the Early Cretaceous and crisis of marine calcifying organisms. Abstracts, 7th International Conference on Paleoceanography (ICP7), 16–22 September, Sapporo, Japan, pp. 117–118.

Herrle, J.O., Mutterlose, J., 2003. Calcareous nannofossils from the Aptian–Lower Albian of southeast France: palaeoecological and biostratigraphic implications. Cretaceous Research 24, 1–22.

Herrle, J.O., Pross, J., Friedrich, O., Kosler, P., Hemleben, C., 2003. Forcing mechanisms for mid-Cretaceous black shale formation: evidence from the Upper Aptian and Lower Albian of the Vocontian Basin (SE France). Palaeogeography, Palaeoclimatology, Palaeoecology 190, 399–426.

Herrle, J.O., Kössler, P., Friedrich, O., Erlenkeuser, H., Hemleben, C., 2004. High resolution carbon isotope records of the Aptian to lower Albian from SE France and the Mazagan Plateau (DSDP Site 545). A stratigraphic tool for paleoceanographic and paleobiologic reconstruction. Earth and Planetary Science Letters 218, 149–161.

Hill, M.E., 1975. Selective dissolution of mid-Cretaceous (Cenomanian) calcareous nannofossils. Micropaleontology 21, 227–235.

Hofmann, P., Stüsser, I., Wagner, T., Schouten, S., Sinnighe Damsté, J.S., 2008. Climate-Ocean coupling off North-West Africa during the Lower Albian: The Oceanic Anoxic Event 1b. Palaeogeography, Palaeoclimatology, Palaeoecology 262, 157–165.

Huber, B.T., Leckie, M., 2011. Planktic foraminiferal species turnover across deep-sea Aptian/Albian boundary sections. Journal of Foraminiferal Research 41, 53–95.

Immenhauser, A., Hillgartner, H., Van Bentum, E., 2005. Microbial foraminiferal episodes in the Early Aptian of the southern Tethyan margin: ecological significance and possible relation to oceanic anoxic event 1a. Sedimentology 52, 77–99.

Jati, M., Grosheny, D., Ferry, S., Masrour, M., Aoutem, M., Içame, N., Gauthier-Lafaye, F., Desmares, D., 2010. The Cenomanian-Turonian boundary event on the Moroccan Atlantic margin (Agadir basin): Stable isotope and sequence stratigraphy. Palaeogeography, Palaeoclimatology, Palaeoecology 296, 151–164.

Jeremiah, J., 1996. A proposed Albian to Lower Cenomanian nannofossil biozonation for England and the North Sea basin. Journal of Micropaleontology 15, 97–129.

Jeremiah, J., 2001. A Lower Cretaceous nannofossil zonation for the North Sea Basin. Journal of Micropaleontology 20, 45–80.

Kilian, W., Gentil, L., 1906. Découverte de deux horizons crétacés remarquables au Maroc. Comptes rendus sommaire de l'Académie des Sciences de Paris 142, 603–605.

Kilian, W., Gentil, L., 1907. Sur les terrains crétacés de l'Atlas Occidental marocain. Comptes rendus sommaire de l'Académie des Sciences de Paris 144, 49–51.

Kuhnt, W., Holbourn, A., Moullade, M., 2011. Transient global cooling at the onset of early Aptian oceanic anoxic event (OAE) 1a. Geology 39, 323–326.

Latil, J.-L., in Chihaoui, A., Jaillard, E., Latil, J.-L., Zghal, I., Susperregi, A.-S., Touir, J., Ouali, J., 2010. Stratigraphy of the Hameima and lower Fahdene Formations in the Tadjerouine area (Northern Tunisia). Journal of African Earth Sciences 58, 387–399.

Latil, J.-L., 2011. Lower Albian ammonites from Central Tunisia and adjacent areas of Algeria. Revue de Paléobiologie 30, 321–429.

Leckie, M., 1984. Mid-Cretaceous planktonic foraminiferal biostratigraphy off central Morocco, Deep Sea Drilling Project Leg 79, sites 545 and 547. In: Hinz, K., Winterer, E.L., et al. (Eds.), 1984. Initial Report of the Deep Sea Drilling Project 79, pp. 579–620.

Leckie, R.M., Bralower, T.J., Cashman, R., 2002. Oceanic anoxic events and plankton evolution: biotic response to tectonic forcing during the mid-Cretaceous. Paleoceanography 17, 13–29.

Lees, J.A., Bown, P.R., Young, J.R., 2006. Photic zone palaeoenvironments of the Kimmeridge Clay Formation (Upper Jurassic, UK) suggested by calcareous nannoplankton palaeoecology; causes and consequence of marine organic carbon burial through time. Palaeogeography, Palaeoclimatology, Palaeoecology 235, 110–134.

Lees, J.A., Bown, P.R., Young, J.R., Riding, J.B., 2004. Evidence for annual records of phytoplankton productivity in the Kimmeridge Clay Formation coccolith stone bands (Upper Jurassic, Dorset, UK); calcareous nannofossil palaeoecology and palaeocenographic reconstructions. Marine Micropaleontology 52, 29–49.

Lemoine, P., 1905. In: Mission dans le Maroc occidental, Automne 1904. Comité du Maroc (Paris), p. 223.

LeRoy, P., Guillocheau, F., Piqué, A., Morabet, A.M., 1998. Subsidence of the Atlantic Moroccan margin during the Mesozoic. Canadian Journal of Earth Sciences 35, 476–493.

Le Roy, P., Piqué, A., 2001. Triassic-Liassic Western Morocco synrift basins in relation to Central Atlantic opening. Marine Geology 172, 359–381.

Linnert, C., Mutterlose, J., Erbacher, J., 2010. Calcareous nannofossils of the Cenomanian/Turonian boundary interval from the Boreal Realm (Wunstorf, northwest Germany). Marine Micropaleontology 74, 38–58.

Masrour, M., Aoutem, M., Atrops, F., 2004. Succession des peuplements d'échinides du Crétacé inférieur dans le Haut Atlas atlantique (Maroc); révision systématique et intérêt stratigraphique. Geobios 37, 595–617.

Mehdi, K., Griboulard, R., Bobier, C., 2004. Rôle de l'halocinèse dans l'évolution du bassin d'Essaouira (Sud-Ouest marocain). Comptes Rendus Géoscience 336, 587–595.

Menegatti, A.P., Weissert, H., Brown, R.S., Tyson, R.V., Farrimond, P., Strasser, A., Caron, M., 1998. High-resolution $\delta^{13}C$ stratigraphy through the early Aptian "Livello Selli" of the Alpine Tethys. Paleoceanography 13, 530–545.

Middlemiss, F.A., 1980. Lower Cretaceous Terbratulidae from South-western Morocco and their biogeography. Paleontology 23, 515–556.

Mutterlose, J., 1989. Temperature-controlled migration of calcareous nannofloras on the north-west European Aptian. In: Crux, J., van Crux, S.E. (Eds.), Nannofossils and their Applications. Ellis Horwood Ltd., Chichester, pp. 122–142.

Mutterlose, J., 1991. Das Verteilungs und Migrationsmuter des kalkigen Nannoplanktons in der borealen Unterkreide (Valangin-Apt). Paläeontographica B 221, 27–152.

Mutterlose, J., Wise Jr., S.W., 1990. Lower Cretaceous nannofossil biostratigraphy of ODP LEG 113 Holes 692B and 693A, continental slope off east Antarctica, Weddell Sea. In: Barker, P.F., Kennett, J.P. (Eds.), 1990. Proceedings of the Ocean Drilling Program, Scientific Results 113, pp. 325–351.

Mutterlose, J., Kessels, K., 2000. Early Cretaceous calcareous nannofossils from high latitudes: implications for palaeobiogeography and palaeoclimate. Palaeogeography, Palaeoclimatology, Palaeoecology 160, 347–372.

Mutterlose, J., Bornemann, A., Luppold, F.W., Owen, H.G., Ruffell, A., Weiss, W., Wray, D., 2003. The Vöhrum section (northwest Germany) and the Aptian/Albian boundary. Cretaceous Research 24, 203–252.

Mutterlose, J., Bornemann, A., Herrle, J., 2009. The Aptian – Albian cold snap: Evidence for "mid" Cretaceous icehouse interludes. Neues Jahrbuch für Geologie und Paläontologie - Abhandlungen 252, 217–225.

Mutti, M., Hallock, P., 2003. Carbonate systems along nutrient and temperature gradients: some sedimentological and geochemical constraint. International Journal of Earth Sciences 92, 465–475.

Nouidar, M., Chellaï, E.H., 2001. Facies and sequence stratigraphy of a Late Barremian wave-dominated deltaic deposit, Agadir Basin, Morocco. Sedimentary Geology 150, 375–384.

Nouidar, M., Chellaï, E.H., 2002. Facies and sequence stratigraphy of an estuarine incised-valley fill: Lower Aptian Bouzergoun Formation, Agadir Basin, Morocco. Cretaceous Research 22, 93–104.

Owen, H.G., 1984. Albian Stage and Substage boundaries. Bulletin of the Geological Society of Denmark 33, 183–189.

Pittet, B., Van Buchem, F.S.P., Hillgärtner, H., Razin, P., Grötsch, J., Droste, H., 2002. Ecological succession, palaeoenvironmental change, and depositional sequences of Barremian-Aptian shallow-water carbonates in northern Oman. Sedimentology 49, 555–581.

Premoli Silvá, I., Erba, E., Tornaghi, M., 1989. Paleoenvironmental signals and changes in surface fertility in Mid Cretaceous Corg-Rich pelagic facies of the Fucoid Marls (Central Italy). Geobios 22, 225–236.

Price, G.D., 2003. New constraints upon isotope variation during the early Cretaceous (Barremian–Cenomanian) from the Pacific Ocean. Geological Magazine 140, 513–522.

Pucéat, E., Lécuyer, C., Sheppard, S.M.F., Dromart, G., Reboulet, S., Grandjean, P., 2003. Thermal evolution of Cretaceous Tethyan marine waters inferred from oxygen isotope composition of fish tooth enamels. Paleoceanography 18, 1029. doi:10.1029/2002PA000823.

Reboulet, S., Mattioli, E., Pittet, B., Baudin, F., Olivero, D., Proux, O., 2003. Ammonoid and nannoplankton abundance in Valanginian (early Cretaceous) limestone-marl successions from the southeast of France basin: carbonate dilution or productivity? Palaeogeography, Palaeoclimatology, Palaeoecology 201, 113–139.

Reboulet, S. (reporter) et al. Report on the 4th International Meeting of the IUGS Lower Cretaceous Ammonite Working Goup, the "Kilian Group" (Dijon, France, 30th August 2010 Cretaceous Research 32, 2011, 786–793.

Rey, J., Canérot, J., Peybernès, B., Taj-Eddine, K., Thieuloy, J.-P., 1988. Lithostratigraphy, biostratigraphy and sedimentary dynamics of the Lower Cretaceous deposits on the northern side of the western High Atlas (Morocco). Cretaceous Research 9, 141–158.

Roch, E., 1930. Histoire stratigraphique du Maroc. Notes et Mémoires du Service géologique du Maroc 80, 440.

Roth, P.H., 1981. Mid-Cretaceous calcareous nannoplankton from the Central Pacific: implications for paleoceanography. In: Thiede, J., et al. (Eds.), 1981. Initial Reports of the Deep Sea Drilling Project 62, pp. 471–489.

Roth, P.H., 1983. Jurassic and Lower Cretaceous calcareous nannofossils in the western North Atlantic (Site 534): biostratigraphy, preservation, and some observations on biogeography and paleoceanography. In: Sheridan, R.E., Gradstein, F.M., et al. (Eds.), 1983. Initial Reports of the Deep Sea Drilling Project 76, pp. 587–621.

Roth, P.H., 1989. Ocean circulation and calcareous nannoplankton evolution during the Jurassic and Cretaceous. Palaeogeography, Palaeoclimatology, Palaeoecology 74, 111–126.

Roth, P.H., Bowdler, J., 1981. Middle Cretaceous nannoplankton biogeography and oceanography of the Atlantic Ocean. In: Warme, J.E., Douglas, R.G., Winterer, E.L. (Eds.), The Deep Sea Drilling Project: a Decade of Progress. Society of Economic Paleontologists and Mineralogists Special Publications 32, pp. 517–546.

Roth, P.H., Krumbach, K.R., 1986. Middle Cretaceous calcareous nannofossil biogeography and preservation in the Atlantic and Indian oceans: implications for paleoceanography. Marine Micropaleontology 10, 235–266.

Rückheim, S., Bornemann, A., Mutterlose, J., 2006a. Integrated stratigraphy of an Early Cretaceous (Barremian – Early Albian) North Sea borehole (BGS 81/40). Cretaceous Research 27, 447–463.

Rückheim, S., Bornemann, A., Mutterlose, J., 2006b. Planktic foraminifera from the mid-Cretaceous (Barremian-EarlyAlbian) of the North Sea Basin: Palaeoecological and palaeoceanographic implications. Marine Micropalaeontology 58, 83–102.

Schlanger, S.O., Jenkyns, H.C., 1976. Cretaceous oceanic anoxic events: causes and consequences. Geologie Mijnbouw 55, 179–184.

Shannon, C.E., Weaver, W., 1949. The Mathematical Theory of Communication. University of Illinois Press, 125 pp.

Street, C., Bown, P., 2000. Palaeobiogeography of Early Cretaceous (Berriasian–Barremian) calcareous nannoplankton. Marine Micropaleontology 39, 265–291.

Takashima, R., Sano, S.I., Iba, Y., Nishi, H., 2007. The first Pacific record of the Late Aptian warming event. Journal of the Geological Society of London 164, 333–339.

Tari, G., Molnar, J., Ashton, P., Hedley, R., October 2000. Salt tectonics in the Atlantic margin of Morocco. The Leading Edge, 1074–1078.

Thielemann, J., 2006. Veränderungen der Levantischen Karbonatplattform in der Mittleren Kreide unter besonderer Berücksichtigung des OAE-1a am Beispiel des Gebel Raghawi, Nordsinai, Ägypten. Diploma Thesis, Univ. Bremen, 91 pp.

Thierstein, H.R., 1980. Selective Dissolution of Late Cretaceous and Earliest Tertiary calcareous nannofossils: experimental evidence. Cretaceous Research 2, 165–176.

Thierstein, H.R., 1981. Late cretaceous nannoplankton and the change at the Cretaceous-Tertiary boundary. In: Society of Economic Paleontologists and Mineralogists Special Publications 32, pp. 355–394.

Wagner, T., Wallmann, K., Herrle, J.O., Hofmann, P., Stuesser, I., 2007. Consequences of moderate 25,000 yr lasting emission of light CO_2 into the mid-Cretaceous ocean. Earth and Planetary Science Letters 259, 200–211.

Wagner, T., Herrle, J.O., Sinninghe Damsté, J., Schouten, S., Stuesser, I., Hofmann, P., 2008. Rapid warming and salinity changes of Cretaceous surface waters in the subtropical North Atlantic. Geology 36, 203–206.

Watkins, D.K., 1989. Nannoplankton productivity fluctuations and rhythmiccally-bedded pelagic carbonates of the Greenhorn Limestone (Upper Cretaceous). Palaeogeography, Palaeoclimatology, Palaeoecology 74, 75–86.

Weissert, H., Lini, A., 1991. Ice age interludes during the time of Cretaceous Greenhouse climate? In: Muller, D.W., McKenzie, J.A., Weissert, H. (Eds.), Controversies in Modern Geology: Evolution of Geological Theories in Sedimentology, Earth History and Tectonics. Academic Press, London, pp. 173–191.

Weissert, H., Lini, A., Föllmi, K.B., Kuhn, O., 1998. Correlation of Early Cretaceous carbon isotope stratigraphy and platform drowning events: a possible link? Palaeogeography Palaeoclimatology, Palaeoecology 137, 189–203.

Weissert, H., Erba, E., 2004. Volcanism, CO_2 and palaeoclimate; a Late Jurassic–Early Cretaceous carbon and oxygen isotope record. Journal of the Geological Society of London 161, 695–702.

Wiedmann, J., Butt, A., Einsele, G., 1978. Vergleich von marokkanischen Kreide-Küstenaufschlüssen and Tiefseebohrungen (D.S.D.P.): Stratigraphie, Paläonenvironment und subsidenz an einem passiven Kontinentalrand. Geologische Runschau 67, 454–508.

Williams, J.R., Bralower, T.J., 1995. Nannofossil assemblages, fine fraction isotopes, and the paleoceanography of the Valanginian–Barremian (Early Cretaceous) North Sea Basin. Paleoceanography 10, 815–839.
Wippich, M.G.E., 2003. Valanginian (Early Cretaceous) ammonite faunas from the western High Atlas, Morocco, and the recognition of western Mediterranean « standard » zones. Cretaceous Research 24, 357–374.
Wise, S.W., 1983. Mesozoic and Cenozoic calcareous nannofossils recovered by DSDP Leg 71 in the Falkland Plateau region, Southwest Atlantic Ocean. In: Ludwig, W.J., Krasheninikov, V., et al. (Eds.), 1983. Initial Reports of the Deep Sea Drilling Project 71, pp. 481–550.
Wise, S.W., 1988. Mesozoic-Cenozoic history of Calcareous Nannofossils in the region of the southern ocean. Palaeogeography, Palaeoclimatology, Palaeoecology 67, 157–179.
Wissler, L., Funk, H., Weissert, H., 2003. Response of Early Cretaceous carbonate platforms to changes in atmospheric carbon dioxide levels. Palaeogeography, Palaeoclimatology, Palaeoecology 200, 187–205.
Witam, O., 1998. Le Barrémien-Aptien de l'Atlas Occidental (Maroc): lithostratigraphie, biostratigraphie, sédimentologie, stratigraphie séquentielle, géodynamique et paléontologie. Strata 30, 1–421.
Wood, R.A., 1993. Nutrients, predation and the history of reef building. Palaios 8, 526–543.
Zühlke, R., Bouaouda, M.-S., Ouajhain, B., Bechstädt, T., Leinfelder, R., 2004. Quantitative Meso/Cenozoic development of the eastern Central Atlantic continental Shelf, western High Atlas, Morocco. Marine and Petroleum Geology 21, 225–276.

Appendix A

The calcium carbonate percent is calculated using the following equations.

Equation 1 (**Measuring CO_2 gas volume**)

$$V\,CO_2 = (V^*(P - Ps)^*273/(760^*(273 + T)$$

Where V is the volume of CO_2 measured in milliliter (ml).

273 K = 0 °C and 760 mmHg (torr) = 1 atm are Standard temperature and pressure (STP).

P: atmospheric pressure obtained using a laboratory barometer in mmHg.

Ps: saturation pressure correction factor (function of temperature) in torr read from table of saturation pressure-temperature data.

T: temperature in Celsius degree obtained using a laboratory thermometer.

Equation 2 (**Weight percent CO_2**)

$$CO_2\,\% = (V\,CO_2{}^*44^*100)/(22{,}414^*M)$$

With 44 = molar mass of CO_2 in $g\cdot mol^{-1}$ and 100 = molar mass of $CaCO_3$ in $g\cdot mol^{-1}$.

At STP, 1 mol of an ideal gas occupies 22,414 ml.

M = weight of sediment powder used (g).

Equation 3 (**Weight percent $CaCO_3$**)

$$CaCO_3\,\% = CO_2\,\%^*2.273^*f$$

With 2.273 = molar mass ratio of $CaCO_3/CO_2$.

f: the correction factor = average ratio between $CaCO_{3mes}\%/CaCO_{3std}\%$ obtained after 5 measurements of the calcium carbonate content ($CaCO_{3mes}$) from a standard ($CaCO_{3std}\% = 98$).

Appendix B

List of nannofossil species recognized in this study

Anfractus harrisonii Medd, 1979
Biscutum constans (Gorka, 1957) Black in Black and Barnes, 1959
Biscutum ellipticum (Gorka, 1957) Grün in Grün and Alleman, 1975
Braarudosphaera africana Stradner, 1961
Braarudosphaera regularis Black, 1973
Broinsonia signata (Noël, 1969) Noël, 1970
Bukrylithus ambiguus Black, 1971
Calculites sp. Jakubowski, 1986
Chiastozygus litterarius (Gorka, 1957) Manivit, 1971
Corollithion signum Stradner, 1962
Cretarhabdus conicus Bramlette and Martini, 1964
Cribrosphaerella ehrenbergii (Arkhangelsky, 1912) Deflandre *in* Piveteau, 1952
Crucibiscutum hayi (Black, 1973) Jakubowski, 1986
Crucibiscutum salebrosum (Black, 1971) Jakubowski, 1986
Cyclagelosphaera margerelii Noël, 1965
Diazomatolithus lehmanii Noël, 1965
Discorhabdus rotatorius (Bukry, 1969) Thierstein, 1973
Eiffelithus striatus Black, 1971
Eprolithus floralis (Stradner, 1962) Stover, 1966
Flabellites oblongus (Bukry, 1969) Crux in Crux et al., 1982
Gaarderella granulifera Black, 1973
Grantarhabdus coronadventis (Reinhardt, 1966) Grün in Grün and Alleman, 1975
Haqius circumradiatus (Stover, 1966) Roth 1978
Hayesites albiensis Manivit, 1971
Hayesites irregularis (Thierstein in Roth and Thierstein, 1972) Applegate, et al., in Covington and Wise, 1987)
Helenea chiastia Worsley, 1971
Hemipodorhabdus gorkae (Reinhardt, 1969) Grün in Grün and Allemann, 1975
Lithraphidites carniolensis Deflandre, 1963
Loxolithus armilla (Black in Black and Barnes, 1959) Noël, 1965
Manivitella pemmatoidea (Deflandre in Manivit, 1965) Thierstein, 1971
Micrantolithus Deflandre in Deflandre and Fert, 1954
Microrhabdulus Deflandre, 1959
Nannoconus inornatus Rutledge and Bown, 1996
Nannoconus quadriangulus Deflandre and Deflandre, 1967
Nannoconus truittii Brönnimann, 1955
Orastrum perspicuum Varol in Al-Rifaiy et al. 1990
Perissocyclus tayloriae Crux, 1989
Placozygus fibuliformis (Reinhardt, 1964) Hoffman, 1970
Polypodorhabdus madingleyensis Black, 1968
Prediscosphaera columnata (Arkhangelsky, 1912) Gartner, 1968
Prediscosphaera spinosa (Bramlette & Martini, 1964) Gartner, 1968
Radiolithus planus Stover, 1966
Repagulum parvidentatum (Deflandre and Fert, 1954) Forchheimer, 1972
Retecapsa surirella (Deflandre and Fert, 1954) Grün in Grün and Allemann, 1975
Rhagodiscus achlyostaurion (Hill, 1976) Doeven, 1983
Rhagodiscus angustus (Stradner, 1963) Reinhardt, 1971
Rhagodiscus asper (Stradner, 1963) Reinhardt, 1967
Rotelapillus lafittei (Noël, 1957) Noël, 1973
Rucinolithus terebrodentarius Applegate, Bralower, Covington and Wise, 1987
Scapholithus Deflandre, in Deflandre and Fert, 1954
Seribiscutum gaultensis Mutterlose, 1992
Sollasites horticus (Stradner et al., 1966) Cepek and Hay, 1969
Staurolithites imbricatus (Gartner, 1968) Burnett, 1997
Staurolithites mitcheneri (Applegate and Bergen, 1988) Rutledge and Bown, 1998
Staurolithites mutterlosei Crux, 1989
Staurolithites siesseri Bown in Kennedy et al., 2000
Stoverius achylosus (Stover, 1966) Perch-Nielsen, 1986
Tegumentum octiformis (Köthe, 1981) Crux, 1989
Tegumentum stradneri Thierstein in Roth and Thierstein, 1972
Tranolithus gabalus Stover, 1966
Tubodiscus Thierstein, 1973
Watznaueria barnesiae (Black 1959) Perch-Nielsen, 1968
Watznaueria biporta Bukry, 1969
Watznaueria britannica (Stradner 1963) Reinhardt, 1964
Watznaueria communis Reinhardt, 1964
Watznaueria fossacincta (Black 1971) Bown in Bown and Cooper 1989
Watznaueria manivitiae Bukry, 1973
Watznaueria ovata Bukry, 1969
Zeugrhabdotus bicrescenticus (Stover, 1966) Burnett in Gale et al., 1996
Zeugrhabdotus diplogrammus (Deflandre in Deflandre and Fert, 1954) Burnett in Gale et al., 1996
Zeugrhabdotus elegans (Gartner, 1968) Burnett in Gale et al., 1996
Zeugrhabdotus embergeri (Noël, 1958) Perch-Nielsen, 1984
Zeugrhabdotus erectus (Deflandre in Deflandre and Fert, 1954) Reinhardt, 1965
Zeugrhabdotus noeliae Rood et al., 1971
Zeugrhabdotus scutula (Bergen, 1994) Rutledge and Bown, 1996
Zeugrhabdotus streetiae Bown in Kennedy et al. 2000
Zeugrhabdotus trivectis Bergen, 1994
Zeugrhabdotus xenotus (Stover, 1966) Burnett in Gale et al., 1996